True Modal Control

A project peport submitted in partial fulfilment of the requirements of the degree of Bachelor of Technology by

Alok Singh (Reg. no. 08010304), and

Murukesh Mohanan (Reg. no. 08010329)

Indian Institute of Technology Guwahati

Department of Mechanical Engineering

April, 2012

Abstract

This project aims to implement True Modal Control, whereby every controllable mode of a dynamic system will be modelled and controlled independently. Dynamic systems can be represented by spring-mass-viscous-damper system via the Lumped Parameter strategy, but we would have to decouple the equations so obtained to obtain the individual modes. Decoupling classically damped systems is easily done, however not much has been done in the case of non-classical damping. We aim to make our method as general as possible, so we shall focus on general damping in this project. There have been recent advances in this field by Garvey et al. (2002a,b) and Chu and Buono (2008a,b). We shall review these advances, and build upon them, principally on the work of Chu and Buono (2008a).

We shall attempt decoupling of coupled second-order dynamic equations. We will take a general quadratic pencil and systematically show how to obtain an equivalent pencil involving diagonal matrices. For this we shall use the concepts of Lancaster Augmented Matrices and Structure Preserving Equivalences (SPEs). The method described in Chu and Buono (2008a) will adapted to handle cases of singular system matrices, with an example of this case presented. The transformations so derived will all be real-valued, keeping in mind that most controllers lack support for complex arimthetic. Then we shall discuss Automorphic (reflexive) SPEs, which enable us to develop stable modal filters.

There are infinitely many Automorphic SPEs, and we shall attempt to ascertain the properties of those which result in stable filters. Exhaustive, sequential evaluation of all grid points as well as Monte Carlo searches have been made for stable filters. The study will include both 2- and 3- dimensional systems. Plots of the Characteristic Polynomial Coefficients (CPCs) of the stable filters provided insight about the space of acceptable automorphic SPEs. Systems in $\mathbb{R}^{2\times 2}$ and $\mathbb{R}^{3\times 3}$ have been examined, since higher order systems are difficult to visualise. A mixed distribution method has been proposed to increase the efficiency of Monte Carlo searches for stable filters.

Acknowledgements

We would like to thank our guide, Dr Karuna Kalita, of the Dept. of Mechanical Engineering in the Indian Institute of Technology Guwahati. Without his insight, remarkable patience and good cheer, the project could not have been completed. We would also like to the thank the various individuals whose research have helped us along the way, in particular, Prof. Garvey, Dr Houlston, and Dr Jiffri of the University of Nottingham, Prof. Chu of the North Carolina State University and Dr del Buono of the University of Bari.

Contents

List of Figures

List of Symbols

Matrices

0 Null matrix. 2, 7–12, 15, 16, 18–20, 35, 36

A LAM comprising **K** and **M**. 7, 10, 11, 15, 16, 35, 36

B LAM comprising **C** and **M**. 10–13, 15, 16, 35, 36

$\mathbf{C}_D$ Diagonalized damping matrix. 11, 12, 14, 37

C Damping matrix. 1, 2, 4, 6–8, 10, 13, 15, 18–20, 22, 23

D LAM comprising **C** and **K**. 15, 16

F Elimination matrix. 11–13, 16, 35, 36

I Identity matrix of size n, $\mathbf{I}_i$ is the identity matrix of size i. 3, 7–11, 13, 15, 16, 18, 19, 22, 35, 36

J Realization matrix. 10–13, 15, 35, 36

$\mathbf{K}_D$ Diagonalized stiffness matrix. 3, 11, 12, 14, 37

K Stiffness matrix. 1–4, 7, 8, 10, 13–16, 18–20, 22, 23

$\mathbf{M}_D$ Diagonalized mass matrix. 3, 11, 12, 14, 15, 37

M Mass matrix. 1–4, 7, 8, 10, 13, 15, 16, 18–20, 22, 23

P Permutation matrix. 11–13, 15, 35, 36

U Right Modal Filter. 22, 23

V Left Modal Filter. 22, 23

X Matrix composed of right eigenvectors. 3, 8, 10–13, 34–39

Y Matrix composed of left eigenvectors. 3, 8, 10, 12, 13, 34–37

Γ Scaling matrix. 11, 13, 36

Λ Diagonal matrix comprising the eigenvalues. 3, 4, 8, 10, 12, 34–37

Π Diagonalizing SPE. 11, 14, 36, 37

γ Diagonal matrix used in decoupling. 9

Operators

$\Im$ Imaginary part of a complex number or matrix. 13

$\Re$ Real part of a complex number or matrix. 13

$[\cdot]^*$ Complex-conjugate or Hermitian transpose of a matrix. 3

$[\cdot]^T$ Transpose of a matrix. 2, 3

$[\cdot]^\dagger$ Moore-Penrose pseudoinverse of a matrix. 12

$|\cdot|$ Determinant of a matrix, Absolute value of a scalar. 3

Other symbols

$L(\lambda)$ Linear matrix pencil. 2, 10, 15

$Q(\lambda)$ Quadratic matrix pencil. 4, 12

$\mathbb{C}^{n\times n}$ The set of complex-valued n-by-n matrices. 3, 9

$\mathbb{R}^{n\times n}$ The set of real-valued n-by-n matrices. 1, 8, 16

$\mathcal{C}\ell_2$ Clifford Algebra over $\mathbb{C}^{n\times n}$. 9

Scalars

ι Imaginary unit. 14, 35–37

λ Eigenvalue. 2–4, 10–12, 14, 15, 34, 37–39

s Laplace complex frequency. 18, 19

Vectors

$\mathbf{\Theta}$ Parameter Vector for Automorphic SPE. 22–24, 28–30

$\mathbf{f}$ Vector of physical forces of the system. 1

$\mathbf{r}$ Vector of physical variables of the system, such as displacements. 1

$\mathbf{x}$ Right eigenvector corresponding to eigenvalue λ. 3

$\mathbf{y}$ Left eigenvector corresponding to eigenvalue λ. 2–4

$\mathfrak{C}$ Index set of complex eigenvectors, $\mathfrak{C}^{+(-)}$ is the index set of complex eigenvectors with positive (negative) imaginary parts. When used as a subscript to a matrix, refers to the submatrix formed from the corresponding index set. 11, 13, 15, 34–37

$\mathfrak{I}$ Index set of purely imaginary eigenvectors, When used as a subscript to a matrix, refers to the submatrix formed from the corresponding index set. 34

$\mathfrak{R}$ Index set of real eigenvectors, When used as a subscript to a matrix, refers to the submatrix formed from the corresponding index set. 34

$\mathfrak{T}$ Index set of real eigenvalues, after classification. $\mathfrak{T}^{+(-)}$ is the index set formed from the first (second) of the index pairs. When used as a subscript to a matrix, refers to the submatrix formed from the corresponding index set. 11, 13, 15, 34, 35, 37, 39

Acronyms

CPC Characteristic Polynomial Coefficient. 1, 22, 23, 28, 29, 31

DOF Degree of Freedom. 1, 20

IMSC Independent Modal Space Control. 5–7

LAM Lancaster Augmented Matrix. 7, 10, 11, 31

MIMSC Modified Independent Modal Space Control. 7

SPE Structure Preserving Equivalence. 1, 7–9, 12–14, 20, 21, 24, 31, 36

Chapter 1

Introduction

Second-order dynamic systems with multiple Degrees of Freedom are very common, and a number of methods have been developed to deal with them. Typically, these systems take the following form:

$$\mathbf{M}\ddot{\mathbf{r}} + \mathbf{C}\dot{\mathbf{r}} + \mathbf{K}\mathbf{r} = \mathbf{f}(t) \tag{1.1}$$

where $\mathbf{r}$, $\mathbf{f} \in \mathbb{R}^n$ are the vector of physical variables, and the vector of external forces respectively and $\mathbf{M}$, $\mathbf{K}$ and $\mathbf{C} \in \mathbb{R}^{n\times n}$. $\mathbf{M}$ may be considered to be the Mass matrix, $\mathbf{C}$ the Damping matrix and $\mathbf{K}$ the Stiffness matrix in analogy with the single DOF spring-mass-viscous-damper system given by the equation (and the corresponding dimensionless form)

$$m\ddot{r} + c\dot{r} + kr = f(t) \tag{1.2a}$$

$$\ddot{r} + 2\zeta\omega\dot{r} + \omega^2 r = g(t) \tag{1.2b}$$

The multi-degree-of-freedom system in Equation 1.1 is usually a coupled system, and the equations are not dimensionless. Hence solving these equations analytically is very difficult, but the equations are usually amenable to numerical solutions. The problem of solving them aside, there is also the vastly more difficult problem of controlling such systems. Manipulating a single physical variable would affect the entire system due to coupling, and the side-effects may be counter-productive. Also, the number of physical quantities in consideration may be more than the number of linearly independent modes of the system. Hence, it is preferable to control the individual *natural modes* of the system, instead of the physical displacements. If the natural modes are independent, as they usually are, the physical displacements are but linear combinations of the modes, one may obtain the needed effect by a proper combination of controlling forces on the modes.

To manipulate the modes, one must first obtain the decoupled equations, since solving these equations yield the modes. Once decoupled, we apply appropriate modal control forces. The decoupled equations must be obtained through *isospectral* transformations, that is, the eigensolution of the coupled and decoupled systems must be the same. Once the forces have been applied, inverse transforms have to be used to obtain the physical

quantities, which will be used in the feedback loop. Whether the system is amenable to decoupling has traditionally been considered to be dependant on the damping matrix $\mathbf{C}$. For the homogeneous system,

$$\mathbf{M}\ddot{\mathbf{r}} + \mathbf{C}\dot{\mathbf{r}} + \mathbf{K}\mathbf{r} = \mathbf{0} \tag{1.3}$$

$\mathbf{C}$ may be zero, the system being undamped. This represents the trivial case and decoupling this is possible due to results dating back to the 19^{th} century.

If the system has *Rayleigh* or *proportional* damping, then $\mathbf{C} = \alpha\mathbf{M} + \beta\mathbf{K}$. The system may have *classical* damping, for which the Caughey-O'Kelly criterion (Caughey and O'Kelly, 1965) applies:

$$\mathbf{C}\mathbf{M}^{-1}\mathbf{K} = \mathbf{K}\mathbf{M}^{-1}\mathbf{C}$$

Rayleigh damping is a special case of classical damping. For classically damped systems, the system maybe decoupled by a simple transformation.

As we shall see, the related eigenvalue problem of the system is quite important in modal analysis and control. Therefore, let us first consider mathematics involved.

1.1 Mathematical Background

Aside from the form presented here, one may also choose to go about using decoupling via the state space form of Equation 1.3. The state space form presents its own eigenvalue problem. However the decoupled equations obtained thus are different from the natural modes. The natural modes would be the equivalents of the dimensionless form (Equation 1.2b). To obtain these, one must diagonalize the system matrices and not the state-space matrices.

1.1.1 No Damping ($\mathbf{C} = \mathbf{0}$)

Equation 1.3 now reduces to

$$\mathbf{M}\ddot{\mathbf{r}} + \mathbf{K}\mathbf{r} = \mathbf{0} \tag{1.4}$$

the corresponding generalized eigenvalue problems being:

$$\mathbf{K}\mathbf{x} = -\lambda\mathbf{M}\mathbf{x}, \tag{1.5a}$$

$$\mathbf{y}^T\mathbf{K} = -\lambda\mathbf{y}^T\mathbf{M}, \tag{1.5b}$$

The eigenvalue problem, when written as a matrix polynomial in λ, is called a pencil, and is termed linear, quadratic, etc. depending on the order of the polynomial. The matrix pencil $L(\lambda)$ in this case is:

$$L(\lambda) := \mathbf{M}\lambda + \mathbf{K} = 0 \tag{1.6}$$

The eigensolution is:

$$\mathbf{\Lambda} = \begin{bmatrix} \lambda_1 & & \\ & \ddots & \\ & & \lambda_n \end{bmatrix} \in \mathbb{C}^{n\times n}, \lambda_1 \geq \ldots \geq \lambda_n \tag{1.7}$$

$$\mathbf{X} = \begin{bmatrix} \mathbf{x}_1 & \ldots & \mathbf{x}_n \end{bmatrix} \in \mathbb{C}^{n\times n} \tag{1.8}$$

$$\mathbf{y} = \begin{bmatrix} \mathbf{y}_1 & \ldots & \mathbf{y}_n \end{bmatrix} \in \mathbb{C}^{n\times n} \tag{1.9}$$

Now, if the matrices $\mathbf{M}$ and $\mathbf{K}$ are symmetric, then we can have $\mathbf{X} = \mathbf{Y}$ but we shall consider the more general, asymmetric, case. For this introduction let us make an assumption, that the system is not defective[1]:

$$|\mathbf{X}| \neq 0 \neq |\mathbf{Y}| \tag{1.10}$$

Traditionally, from this point on, one would usually encounter similarity transformations (Watkins, 2010). Thus:

$$\mathbf{M}_D = \mathbf{X}^{-1}\mathbf{M}\mathbf{X} \tag{1.11}$$

$$\mathbf{K}_D = \mathbf{X}^{-1}\mathbf{K}\mathbf{X} \tag{1.12}$$

If the matrices were special in some way, say, if they were *normal*[2], one would expect some unitary similarity transformations[3]. Or, if they were symmetric, which is often the case, orthogonal transformations ($\mathbf{X}^T\mathbf{X} = \mathbf{I}$):

$$\mathbf{M}_D = \mathbf{X}^T\mathbf{M}\mathbf{X} \tag{1.13}$$

$$\mathbf{K}_D = \mathbf{X}^T\mathbf{K}\mathbf{X} \tag{1.14}$$

However, let us depart from the traditional way, and inspect the use of both left and right eigenvectors. It turns out that we can diagonalize $\mathbf{M}$ and $\mathbf{K}$ by the *isospectral* transformations (Chu and Buono, 2008a)

$$\mathbf{M}_D = \mathbf{Y}^T\mathbf{M}\mathbf{X} \tag{1.15}$$

$$\mathbf{K}_D = \mathbf{Y}^T\mathbf{K}\mathbf{X} \tag{1.16}$$

The term isospectral is used in the strong sense that the eigenvalues and all their partial multiplicities are common to isospectral systems. Note that all similarity transforms are isospectral, but the converse is not necessarily true. Now, if the eigenvectors given by $\mathbf{X}$ and $\mathbf{Y}$ are normalized, we have,

$$\mathbf{I} = \mathbf{Y}^T\mathbf{M}\mathbf{X} \tag{1.17a}$$

$$\mathbf{\Lambda} = \mathbf{Y}^T\mathbf{K}\mathbf{X} \tag{1.17b}$$

yielding the decoupled equations

$$\ddot{\mathbf{q}} + \lambda\mathbf{q} = \mathbf{0}, \quad \mathbf{q} = \mathbf{X}\mathbf{r}$$

which represent the individual modes of the system.

[1] A system with n eigenvalues is defective iff it does not have n linearly independent eigenvectors.

[2] Matrix $\mathbf{A}$ is said to be normal iff $\mathbf{A}\mathbf{A}^* = \mathbf{A}^*\mathbf{A}$.

[3] If $\mathbf{U} \in \mathbb{C}^{n\times n}$ is a unitary matrix, $\mathbf{U}^*\mathbf{U} = \mathbf{U}\mathbf{U}^* = \mathbf{I}$. Orthogonal matrices are real unitary matrices.

1.1.2 Classical Damping

For classically damped systems, the eigenvalue problem remains unchanged. Further, the transformations that diagonalize $\mathbf{M}$ and $\mathbf{K}$ (Equation 1.17) also diagonalize $\mathbf{C}$. This is trivially so for Rayleigh damping. The proof is not of essence to our task, so it shall not be stated here. However those interested may consult Inman (2001) for a short proof that the Caughey-O'Kelly criterion is the necessary and sufficient condition for this.

1.1.3 General damping

In the event that damping is not classical, the transformations are not guaranteed to simultaneously diagonalize all three matrices. In particular, gyroscopic systems have skew-symmetric damping matrices. The eigenvalue problem is also different. It is no longer linear, but quadratic:

$$(\mathbf{M}\lambda^2 + \mathbf{C}\lambda + \mathbf{K})\mathbf{x} = 0 \tag{1.18a}$$

$$\mathbf{y}^T(\mathbf{M}\lambda^2 + \mathbf{C}\lambda + \mathbf{K}) = 0 \tag{1.18b}$$

$$Q(\lambda) := \mathbf{M}\lambda^2 + \mathbf{C}\lambda + \mathbf{K} = 0 \tag{1.18c}$$

This eigenvalue problem, is no longer n-dimensional, but $2n$-dimensional, since there are $2n$ eigenvalues which satisfy the quadratic pencil. Hence the computational complexity of the problem becomes considerably higher.

1.1.4 Defective systems

We made an assumption that the system is not defective (Equation 1.10). Defective matrices are rare enough that one is justified in making this assumption. Defective matrices may not be fully diagonalized, but they can be converted into the Jordan normal form:

$$\mathbf{\Lambda} = \begin{bmatrix} \mathbf{\Lambda}_1 & & & \\ & \mathbf{\Lambda}_2 & & \\ & & \ddots & \\ & & & \mathbf{\Lambda}_n \end{bmatrix} \tag{1.19}$$

$$\mathbf{\Lambda}_i = \begin{bmatrix} \lambda_i & 1 & & \\ & \lambda_i & \ddots & \\ & & \ddots & 1 \\ & & & \lambda_i \end{bmatrix} \tag{1.20}$$

The $\mathbf{\Lambda}_i$ are called Jordan blocks. The number of Jordan blocks for an eigenvalue is its geometric multiplicity, and the sum of the sizes of the blocks is its algebraic multiplicity. The matrix is diagonalizable iff both multiplicities are same for all eigenvalues. If this is not the case, then the modes involving a common eigenvalue might be coupled with each

other, as they are not independent. Defective systems are very sensitive to perturbation, and even systems close to defective matrices suffer from this problem. Therefore an error in computation, due to round-off error, or truncation, can change the characteristics of the problem.

1.2 Modal Control in General

Modal Control enjoyed its heyday in the 1980s and 1990s. Then it fell out of favour, due to problems involving uncontrolled modes and spillover, which we shall discuss in the next chapter. Another major drawback was the requirement of a large number of sensors to monitor all the modes. Further, Independent Modal Space Control (IMSC) and other methods are not suited for problems involving gyroscopic systems. Meirovitch and Ryland II (1979) has presented improvements in IMSC which handle gyroscopic systems with slight damping, a restriction which we seek to remove. The Caughey-O'Kelly criterion has been called into question, and qualifications added (Phani, 2003). Thus, there is a need for general decoupling transformations.

However, not only do we need general decoupling transformations, we need *real-valued* transformations. Complex transforms, while mathematically convenient to obtain, add a layer of complexity in practical computation. The Caughey-O'Kelly condition, insofar as it holds, do provide for such transformations, from results known to mathematicians from the times of Weierstrass. Another requirement is that the transformations be *stable*. Stability can be considered in two contexts – numerical stability and stability of the eigensystem with respect to perturbation. If the transforms are not numerically stable, errors in the system will be magnified, and attempts at control will prove expensive and ineffectual. Since modal control aims to modify the modes, i.e., the eigenvalues and eigenvectors, unstable perturbations of the eigensystem would prove counter-productive.

1.2.1 True Modal Control

True Modal Control aims to use such general decoupling transformations to completely decouple systems with arbitrary damping. Then each mode shall be controlled independently, such that the overall effect is to coerce the physical variables to the desired state. The transformations involved would be real-valued. Thus, True Modal Control will address the problems of spillover, since all modes will be modelled. Further, characteristics of the system such as gyroscopic damping, which often proves stabilizing, would be retained, and put to use in an advantageous manner.

There have been recent advances in this field by Garvey et al. (2002a,b) and Chu and Buono (2008a,b). This project aims to build on and improve their results, both in a mathematical sense and in a computational sense. One case that is side-stepped by current strategies is a zero eigenvalue, or, equivalently, a system with rigid-body modes. Accommodating this case and that of defective systems is another goal of this project. We shall discuss these and the various modal control strategies in the next chapter.

Chapter 2

Literature Review

Theories on Modal Control have been around for around half a century, initially suggested by Rosenbrock (1962). Simon and Mitter (1968) expanded on this work. Modal control theories emerged independently in two fields - chemical engineering, and structural dynamics. The concepts which evolved in structural engineering were formulated into IMSC by Prof Meirovitch and his team in the 1980s, and this work has been summarized in Meirovitch (1990).

2.1 Independent Modal Space Control

In IMSC, one decouples the equations (1.1) by unitary similarity transforms. In the event that $\mathbf{C}$ is not diagonalized, we ignore the off-diagonal terms. Further, the control forces are only applied to the lower modes, since the higher modes are difficult to physically monitor or control. Thus, IMSC is most effective in situations where only a few critical modes need be studied and controlled. However, this strategy exposes itself by two grievous flaws in the general case. Firstly, when the off-diagonal terms are of comparable magnitude to the diagonal terms, ignoring them is a very poor approximation. In rotating systems, for example, the skew-symmetry of the damping matrix is due to the gyroscopic nature of the system, and ignoring off-diagonal terms here is ignoring the gyroscopic effects themselves – and the very essence of the problem. It may happen that the decoupled equations thus obtained have quite different eigenvalues from the original. There is also the problem of deciding how many modes one must model, how many to leave unmodelled, and how many of the modelled modes be controlled. This question is further complicated by the different needs of open and closed loop control systems. What may be satisfactory for one may not be so for the other.

Secondly, trying to control only the lower modes raises the problem of spill-over. Spill-over refers to applying a control law designed around a limited model of a system, to the entire system and inadvertently exciting that part of the model discarded (called residual modes in a modal model of a structure). Since the higher modes are not in the model, the effect will be different from that predicted by the control design. In some cases, the

modal control forces may significantly increase the contributions of uncontrolled modes to the vibration of the system, especially in cases like flexible structures, in which the contributions of its higher modes cannot be ignored. Thus while using a modal model one must be careful not to excite the unused modes with the control system designed to improve the structure's response. Otherwise, control energy will 'spill over' into the residual modes and excite these modes, spoiling the response and desired performance is not achieved.

As mentioned earlier, IMSC converts the n-DOF second-order system to a $2n$-DOF first-order system. That is, the system is linearised. Useful characteristics of the system matrices such as symmetry and definiteness are lost. A Modified Independent Modal Space Control (MIMSC) theory as presented by Fang et al. (2003) seeks to address shortcomings of IMSC, such as spill over.

2.2 Structure Preserving Equivalences (SPEs)

The quadratic pencil (1.18c) can be linearized to different forms. Consider the following matrices, called Lancaster Augmented Matrices:

$$\mathbf{A} = \begin{bmatrix} \mathbf{K} & \mathbf{0} \\ \mathbf{0} & -\mathbf{M} \end{bmatrix} \quad \mathbf{B} = \begin{bmatrix} \mathbf{C} & \mathbf{M} \\ \mathbf{M} & \mathbf{0} \end{bmatrix} \quad \mathbf{D} = \begin{bmatrix} \mathbf{0} & \mathbf{K} \\ \mathbf{K} & \mathbf{C} \end{bmatrix} \tag{2.1}$$

and the *companion matrices*, often seen in the state-space form of system equations:

$$\mathbf{C}_R = \begin{bmatrix} \mathbf{0} & \mathbf{I} \\ -\mathbf{M}^{-1}\mathbf{K} & -\mathbf{M}^{-1}\mathbf{C} \end{bmatrix} \qquad \mathbf{C}_L = \begin{bmatrix} \mathbf{0} & \mathbf{K}\mathbf{M}^{-1} \\ \mathbf{I} & \mathbf{C}\mathbf{M}^{-1} \end{bmatrix} \tag{2.2}$$

If we let $\mathbf{p} = \dot{\mathbf{r}}$ and $\mathbf{P} = \dot{\mathbf{f}}$, then we can write equation (1.1) in any of the following state-space forms:

$$\mathbf{D}\begin{bmatrix} \mathbf{r} \\ \mathbf{p} \end{bmatrix} - \mathbf{A}\begin{bmatrix} \dot{\mathbf{r}} \\ \dot{\mathbf{p}} \end{bmatrix} = \begin{bmatrix} \mathbf{0} \\ \mathbf{I} \end{bmatrix} \mathbf{f} \tag{2.3}$$

$$\mathbf{A}\begin{bmatrix} \mathbf{r} \\ \mathbf{p} \end{bmatrix} + \mathbf{B}\begin{bmatrix} \dot{\mathbf{r}} \\ \dot{\mathbf{p}} \end{bmatrix} = \begin{bmatrix} \mathbf{I} \\ \mathbf{0} \end{bmatrix} \mathbf{f} \tag{2.4}$$

$$\mathbf{D}\begin{bmatrix} \mathbf{r} \\ \mathbf{p} \end{bmatrix} + \mathbf{B}\begin{bmatrix} \dot{\mathbf{r}} \\ \dot{\mathbf{p}} \end{bmatrix} = \begin{bmatrix} \mathbf{P} \\ \mathbf{f} \end{bmatrix} \tag{2.5}$$

Now, two non-singular matrices T_L and $T_R \in \mathbb{C}^{2n\times 2n}$, can be considered to be SPEs[1], if the isospectral transforms $\mathbf{A}_0 = \mathbf{T}_L\mathbf{A_0}\mathbf{T}_R, \mathbf{B}_0 = \mathbf{T}_L\mathbf{B_0}\mathbf{T}_R$ and $\mathbf{D}_0 = \mathbf{T}_L\mathbf{D_0}\mathbf{T}_R$, retain their block-structure, that is, if

$$\mathbf{A_0} = \begin{bmatrix} \mathbf{K}_0 & \mathbf{0} \\ \mathbf{0} & -\mathbf{M}_0 \end{bmatrix} \quad \mathbf{B_0} = \begin{bmatrix} \mathbf{C}_0 & \mathbf{M}_0 \\ \mathbf{M}_0 & \mathbf{0} \end{bmatrix} \quad \mathbf{D}_0 = \begin{bmatrix} \mathbf{0} & \mathbf{K}_0 \\ \mathbf{K}_0 & \mathbf{C}_0 \end{bmatrix} \tag{2.6}$$

[1]As used by Garvey et al. (2002a,b), there is a restriction on the above definition: that $\mathbf{M}_0$ not be singular. We shall modify this restriction: $\mathbf{M}_0 \neq \mathbf{0}$. The reason shall be apparent later.

Utilisation of the SPEs permits the diagonalization of the system mass, damping and stiffness matrices for non-classically damped systems, as shown by Garvey et al. (2002a,b). A modal control method is presented by Houlston (2007), which exploits this diagonalization. The method introduces independent modal control in which a separate modal controller is designed in modal space for each individual mode or pair of modes. The theory of decoupling used is presented in a concise form in Garvey et al. (2001). We shall present the basic equations here.

Except for defective systems, it is possible to find matrices $\mathbf{W}_L$, $\mathbf{X}_L$, $\mathbf{Y}_L$, $\mathbf{Z}_L$ and $\mathbf{W}_R$, $\mathbf{X}_R$, $\mathbf{Y}_R$, $\mathbf{Z}_R$ in $\mathbb{R}^{n\times n}$ such that

$$\begin{bmatrix}\mathbf{W}_L & \mathbf{X}_L\\ \mathbf{Y}_L & \mathbf{Z}_L\end{bmatrix}^T \begin{bmatrix}\mathbf{0} & \mathbf{K}\\ \mathbf{K} & \mathbf{C}\end{bmatrix} \begin{bmatrix}\mathbf{W}_R & \mathbf{X}_R\\ \mathbf{Y}_R & \mathbf{Z}_R\end{bmatrix} = \begin{bmatrix}\mathbf{0} & \mathbf{\Omega}^2\\ \mathbf{\Omega}^2 & (2\zeta\mathbf{\Omega})\end{bmatrix} \tag{2.7}$$

$$\begin{bmatrix}\mathbf{W}_L & \mathbf{X}_L\\ \mathbf{Y}_L & \mathbf{Z}_L\end{bmatrix}^T \begin{bmatrix}\mathbf{K} & \mathbf{0}\\ \mathbf{0} & -\mathbf{M}\end{bmatrix} \begin{bmatrix}\mathbf{W}_R & \mathbf{X}_R\\ \mathbf{Y}_R & \mathbf{Z}_R\end{bmatrix} = \begin{bmatrix}\mathbf{\Omega}^2 & \mathbf{0}\\ \mathbf{0} & -\mathbf{I}\end{bmatrix} \tag{2.8}$$

$$\begin{bmatrix}\mathbf{W}_L & \mathbf{X}_L\\ \mathbf{Y}_L & \mathbf{Z}_L\end{bmatrix}^T \begin{bmatrix}\mathbf{C} & \mathbf{M}\\ \mathbf{M} & \mathbf{0}\end{bmatrix} \begin{bmatrix}\mathbf{W}_R & \mathbf{X}_R\\ \mathbf{Y}_R & \mathbf{Z}_R\end{bmatrix} = \begin{bmatrix}(2\zeta\mathbf{\Omega}) & \mathbf{I}\\ \mathbf{I} & \mathbf{0}\end{bmatrix} \tag{2.9}$$

where, both $\mathbf{\Omega}^2$ and $2\zeta\mathbf{\Omega}$ are real-valued and diagonal. Now,

$$\mathbf{Y}_L = -\mathbf{X}_L\mathbf{\Omega}^2, \quad \mathbf{W}_L = \mathbf{Z}_L + \mathbf{X}_L(2\zeta\mathbf{\Omega}) \tag{2.10}$$

A similar relation holds for the right matrices. Consider the eigenvalue problem obtained from the first of the state-space forms in (2.3). Let $\mathbf{X}$ be the matrix composed of right eigenvectors and $\mathbf{Y}$ be the matrix composed of left eigenvectors. Considering a block structure using matrices similar to $\mathbf{W}_L$, $\mathbf{X}_L$, $\mathbf{Y}_L$,, etc., let $\mathbf{\Phi}_{L1}$, $\mathbf{\Phi}_{L2}$, $\mathbf{\Theta}_{L2}$, $\mathbf{\Theta}_{L2}$ form the block structure of $\mathbf{X}$, with a similar structure for $\mathbf{Y}$. Then, rewriting (1.17) using the block structure:

$$\begin{bmatrix}\mathbf{\Phi}_{L1} & \mathbf{\Phi}_{L2}\\ \mathbf{\Theta}_{L1} & \mathbf{\Theta}_{L2}\end{bmatrix}^T \begin{bmatrix}\mathbf{0} & \mathbf{K}\\ \mathbf{K} & \mathbf{C}\end{bmatrix} \begin{bmatrix}\mathbf{\Phi}_{R1} & \mathbf{\Phi}_{R2}\\ \mathbf{\Theta}_{R1} & \mathbf{\Theta}_{R2}\end{bmatrix} = \begin{bmatrix}\mathbf{\Lambda}_1 & \mathbf{0}\\ \mathbf{0} & \mathbf{\Lambda}_2\end{bmatrix} \tag{2.11}$$

$$\begin{bmatrix}\mathbf{\Phi}_{L1} & \mathbf{\Phi}_{L2}\\ \mathbf{\Theta}_{L1} & \mathbf{\Theta}_{L2}\end{bmatrix}^T \begin{bmatrix}\mathbf{K} & \mathbf{0}\\ \mathbf{0} & -\mathbf{M}\end{bmatrix} \begin{bmatrix}\mathbf{\Phi}_{R1} & \mathbf{\Phi}_{R2}\\ \mathbf{\Theta}_{R1} & \mathbf{\Theta}_{R2}\end{bmatrix} = \begin{bmatrix}\mathbf{I} & \mathbf{0}\\ \mathbf{0} & \mathbf{I}\end{bmatrix} \tag{2.12}$$

Of the $2n$ eigenvalues obtained, counting multiplicity, let $2p \leq 2n$ be the number of complex eigenvalues with $2q$ real eigenvalues. The matrix which we now define will also be used later, since a modified version plays the same role in the theory presented by Chu and Buono (2008a).

$$\mathbf{J} = \begin{bmatrix}\frac{1}{\sqrt{2}}\mathbf{I}_p & \mathbf{0} & \frac{-\iota}{\sqrt{2}}\mathbf{I}_p & \mathbf{0}\\ \mathbf{0} & \mathbf{I}_q & \mathbf{0} & \mathbf{0}\\ \frac{1}{\sqrt{2}}\mathbf{I}_p & \mathbf{0} & \frac{\iota}{\sqrt{2}}\mathbf{I}_p & \mathbf{0}\\ \mathbf{0} & \mathbf{0} & \mathbf{0} & \iota\mathbf{I}_q\end{bmatrix} \tag{2.13}$$

$$\mathbf{J}^T\mathbf{\Lambda}\mathbf{J} = \begin{bmatrix}\mathbf{\Lambda}_x & \mathbf{\Lambda}_y\\ \mathbf{\Lambda}_y & \mathbf{\Lambda}_z\end{bmatrix} \tag{2.14}$$

Now select a diagonal matrix $\gamma \in \mathbb{C}^{n\times n}$, such that

$$\begin{bmatrix}\cosh\gamma & \sinh\gamma\\ \sinh\gamma & \cosh\gamma\end{bmatrix}\begin{bmatrix}\mathbf{\Lambda}_x & \mathbf{\Lambda}_y\\ \mathbf{\Lambda}_y & \mathbf{\Lambda}_z\end{bmatrix}\begin{bmatrix}\cosh\gamma & \sinh\gamma\\ \sinh\gamma & \cosh\gamma\end{bmatrix} = \begin{bmatrix}\mathbf{0} & \mathbf{\Omega}^2\\ \mathbf{\Omega}^2 & (2\zeta\mathbf{\Omega})\end{bmatrix} \tag{2.15}$$

Then the following relation (with its equivalent for the right eigenvectors) give us the required diagonalizing SPEs:

$$\begin{bmatrix}\mathbf{W}_L & \mathbf{X}_L\\ \mathbf{Y}_L & \mathbf{Z}_L\end{bmatrix} = \begin{bmatrix}\mathbf{\Phi}_{L1} & \mathbf{\Phi}_{L2}\\ \mathbf{\Theta}_{L1} & \mathbf{\Theta}_{L2}\end{bmatrix}\mathbf{J}\begin{bmatrix}\cosh\gamma & \sinh\gamma\\ \sinh\gamma & \cosh\gamma\end{bmatrix}\begin{bmatrix}\mathbf{\Omega} & \mathbf{0}\\ \mathbf{0} & \mathbf{I}\end{bmatrix} \tag{2.16}$$

There are two points to consider in this rather straightforward relation. First is obtaining an appropriate γ, which is where the bulk of the computation lies. Secondly, there is no simple way whereby this method could be adapted for systems with eigenvalue zero. Chu and Buono (2008a) derived a modified version of this relation, which, as we shall show in the next chapter, is relatively easily adapted for this case. The transformation derived above is not unique, and can be arrived via a different route, albeit sharing a few steps. Another route to decoupling transformations is also discussed in Garvey et al. (2001), which uses Clifford algebra, specifically, $\mathcal{C}\ell_2$. We shall not discuss this method, since Clifford algebras are beyond the scope of this work.

Chapter 3

Total Decoupling

In this chapter, we shall first describe the diagonalizing transformations derived by Chu and Buono (2008a), followed by the modifications needed for handling the case when zero is an eigenvalue. Then we shall have a brief discussion of the computational complexity involved and measures to decrease it. Before we start, let us a have brief overview of the symbols used, which were previously introduced. We shall be using the LAMs $\mathbf{A}$ and $\mathbf{B}$, with the corresponding matrix pencil $L(\lambda)$ and eigensystem $\mathbf{\Lambda}$, $\mathbf{X}$ and $\mathbf{Y} \in \mathbb{C}^{2n\times 2n}$:

$$\mathbf{A} = \begin{bmatrix} -\mathbf{K} & \mathbf{0} \\ \mathbf{0} & \mathbf{M} \end{bmatrix} \tag{3.1}$$

$$\mathbf{B} = \begin{bmatrix} \mathbf{C} & \mathbf{M} \\ \mathbf{M} & \mathbf{0} \end{bmatrix} \tag{3.2}$$

$$L(\lambda) := \mathbf{B}\lambda - \mathbf{A} = 0 \tag{3.3}$$

Except for $\mathbf{J}$, we shall not be using the matrices defined in section 2.2. We are using normalized eigenvectors, so that:

$$\mathbf{Y}^T\mathbf{A}\mathbf{X} = \mathbf{\Lambda} \tag{3.4a}$$

$$\mathbf{Y}^T\mathbf{B}\mathbf{X} = \mathbf{I}_{2n} \tag{3.4b}$$

Now let us scale the eigenvectors by their eigenvalues, thus:

$$\mathbf{X}^{[1]} = \mathbf{X}\mathbf{\Lambda}^{-1/2} \tag{3.5}$$

$$\mathbf{Y}^{[1]} = \mathbf{Y}\mathbf{\Lambda}^{-1/2} \tag{3.6}$$

Since $\mathbf{\Lambda}$ is a diagonal matrix, its inverse is obtained by taking the reciprocals of its diagonal elements. The principle square root of the diagonal elements is used. Then (3.4) becomes

$$\mathbf{Y}^{[1]T}\mathbf{A}\mathbf{X}^{[1]} = \mathbf{I}_{2n} \tag{3.7a}$$

$$\mathbf{Y}^{[1]T}\mathbf{B}\mathbf{X}^{[1]} = \mathbf{\Lambda}^{-1} \tag{3.7b}$$

The remaining steps belong to three stages: classification of the eigenvalues and their eigenvectors, elimination of complex values and scaling to restore the transformed $\mathbf{A}$ and $\mathbf{B}$ to LAMs. The classification procedure and the derivation of the other matrices are provided in Appendix Appendix A. For now, we shall simply state the key matrices obtained:

$$\mathbf{P} = \mathbf{I}_{2n}\left[\mathfrak{C}^{+}\mathfrak{T}^{+}\mathfrak{C}^{-}\mathfrak{T}^{-}\right] \tag{3.8a}$$

$$\mathbf{J}_L = \begin{bmatrix} \frac{1}{\sqrt{2}}\mathbf{I}_p & \mathbf{0} & \frac{-\iota}{\sqrt{2}}\mathbf{I}_p & \mathbf{0} \\ \mathbf{0} & \mathbf{L}^{+} & \mathbf{0} & \mathbf{0} \\ \frac{1}{\sqrt{2}}\mathbf{I}_p & \mathbf{0} & \frac{\iota}{\sqrt{2}}\mathbf{I}_p & \mathbf{0} \\ \mathbf{0} & \mathbf{0} & \mathbf{0} & \mathbf{L}^{-} \end{bmatrix} \tag{3.8b}$$

$$\mathbf{J}_R = \begin{bmatrix} \frac{1}{\sqrt{2}}\mathbf{I}_p & \mathbf{0} & \frac{-\iota}{\sqrt{2}}\mathbf{I}_p & \mathbf{0} \\ \mathbf{0} & \mathbf{R}^{+} & \mathbf{0} & \mathbf{0} \\ \frac{1}{\sqrt{2}}\mathbf{I}_p & \mathbf{0} & \frac{\iota}{\sqrt{2}}\mathbf{I}_p & \mathbf{0} \\ \mathbf{0} & \mathbf{0} & \mathbf{0} & \mathbf{R}^{-} \end{bmatrix} \tag{3.8c}$$

$$\mathbf{F} = \begin{bmatrix} \mathbf{\Phi} & \mathbf{0} & \mathbf{I}_p & \mathbf{0} \\ \mathbf{0} & \mathbf{\Psi}^{+} & \mathbf{0} & \mathbf{I}_{n-p} \\ \mathbf{I}_p & \mathbf{0} & \mathbf{\Phi} & \mathbf{0} \\ \mathbf{0} & \mathbf{I}_{n-p} & \mathbf{0} & \mathbf{\Psi}^{-} \end{bmatrix} \tag{3.8d}$$

$$\mathbf{\Gamma} = \begin{bmatrix} \mathbf{I}_n & \mathbf{0} \\ \mathbf{0} & \mathbf{\Theta} \end{bmatrix} \tag{3.8e}$$

which give us the diagonalizing transformations $\mathbf{\Pi}_L$ and $\mathbf{\Pi}_R$:

$$\mathbf{\Pi}_L = \mathbf{X}^{[1]}\mathbf{P}\mathbf{J}_L\mathbf{F}\mathbf{\Gamma} \tag{3.9a}$$

$$\mathbf{\Pi}_R = \mathbf{X}^{[1]}\mathbf{P}\mathbf{J}_R\mathbf{F}\mathbf{\Gamma} \tag{3.9b}$$

$\mathbf{\Pi}_L$ and $\mathbf{\Pi}_R$ give us the diagonalized system — $\mathbf{K}_D$, $\mathbf{M}_D$ and $\mathbf{C}_D$:

$$\mathbf{\Pi}_L^T\mathbf{A}\mathbf{\Pi}_R = \begin{bmatrix} \mathbf{K}_D & \mathbf{0} \\ \mathbf{0} & \mathbf{M}_D \end{bmatrix} \tag{3.10a}$$

$$\mathbf{\Pi}_L^T\mathbf{B}\mathbf{\Pi}_R = \begin{bmatrix} \mathbf{0} & \mathbf{M}_D \\ \mathbf{M}_D & \mathbf{C}_D \end{bmatrix} \tag{3.10b}$$

3.1 Modifications

Consider the case when $\lambda_i = 0$, for some $1 \leq i \leq 2n$. Then, the algorithm fails when at the very beginning, when scaling the eigenvectors using the eigenvalues (3.5). The matrix form of the equation immediately suggests an alternate route. Pseudo-inverses of singular matrices are very well known and well-defined. Therefore, we use the pseudo-inverse of the matrix of eigenvalues, specifically the Moore-Penrose pseudo-inverse. The inverse of a diagonal matrix is also a diagonal matrix with reciprocals of the corresponding diagonal

terms. The pseudo-inverse of a singular diagonal matrix (obviously having atleast one zero in the diagonal), is also a diagonal matrix with reciprocals of the corresponding diagonal terms, except for the zeros, which remain zero. Thus:

$$\begin{bmatrix} \mathbf{\Lambda}_1 & & \\ & \mathbf{0} & \\ & & \mathbf{\Lambda}_2 \end{bmatrix}^{\dagger} = \begin{bmatrix} \mathbf{\Lambda}_1^{-1} & & \\ & \mathbf{0} & \\ & & \mathbf{\Lambda}_2^{-1} \end{bmatrix} \tag{3.11}$$

Therefore, when we scale the eigenvectors using the pseudo-inverse, the columns of $\mathbf{X}$ and $\mathbf{Y}$ corresponding to the eigenvalue zero become zero themselves. Whenever the inverse of a singular matrix is needed in the equations, we shall use the pseudo-inverse instead. This may happen in the equations (A.22), (A.25) and (A.28). The next problem arising when a $\lambda_i = 0$ is in the classification of eigenvalues (see Appendix A). Here we may relax one each of the three pairs of strict inequalities. The choice is quite arbitrary, since the use pseudo-inverses means that any cases division by 0 would be have a result equivalent to multiplication 0. In any case, one must check for small non-zero values that maybe result of round-off errors and truncation errors. These values should rightly be exactly zero, but often aren't, and dividing by these small values should be avoided.

Now let us consider the implications of using the pseudo-inverse. Since the the transformations represented by $\mathbf{P}$, $\mathbf{J}$ and $\mathbf{F}$ are linear combinations of the scaled eigenvectors, the final SPEs obtained do not have full rank, and hence are not invertible. But, the filters obtained from these SPEs can be made invertible, using the concept of stable filters discussed in the next chapter. Consider the quadratic pencil $Q(\lambda)$ (1.18c), now using the diagonalized matrices $\mathbf{K}_D$, $\mathbf{M}_D$ and $\mathbf{C}_D$. Then we can write the pencil as separate polynomials in λ. If zero satisfies one of these polynomials, as it should, then one would expect that one of the diagonal elements in $\mathbf{K}_D$ is zero. For each repeated occurrence of zero as an eigenvalue, a diagonal element in $\mathbf{K}_D$ would be zero.

Unexpectedly, this is not what happens. Instead of ending up in $\mathbf{K}_D$, the zeros end up in $\mathbf{M}_D$. Effectively, this means that, for each multiplicity of zero as an eigenvalue, one of the decoupled polynomial reduces its degree from quadratic to linear. The reduced polynomials have a non-zero real eigenvalue as their root. Also, the corresponding equation of motion now lacks an acceleration term! Studying the implications of this could be a goal of future research.

3.2 Computational Improvements

Like complex numbers, matrices are convenient for mathematics and rather inconvenient for computation. Multiplying two square matrices of size n is an $O(n^3)$ task. Hence, while it is convenient to write $\mathbf{X}^{[1]} = \mathbf{XP}$, for the purpose of computation, selecting the individual columns is much faster. Also, the original equations presented in Chu and Buono (2008a) use arbitrary eigenvectors, and scale them via the matrix multiplication $\mathbf{X}^{[1]} = \mathbf{X}\mathbf{B}_1^{-1/2}$, and $\mathbf{Y}^{[1]} = \mathbf{Y}\mathbf{B}_1^{-1/2}$, where $\mathbf{B}_1 = \mathbf{Y}^T\mathbf{B}\mathbf{X}$. This involves 4 matrix multiplications, whereas

solving for $\mathbf{Y}$ in the equation

$$\mathbf{I}_{2n} = \mathbf{Y}^T\mathbf{B}\mathbf{X} \tag{3.12}$$

gives us $\mathbf{Y} = (\mathbf{X}\mathbf{B})^{-T}$, which saves us two matrix multiplications and the cost of calculating the left eigenvectors of the system.

From similar arguments, the role of $\mathbf{J}_R$, and $\mathbf{J}_L$, can be eliminated, reducing the matrix multiplications to obtaining multiples of eigenvectors or obtaining real or imaginary parts of the eigenvectors, for example[1]:

$$\begin{aligned}
\mathbf{X}^{[2]} &= \mathbf{X}\mathbf{P}\mathbf{J}_R \\
&= \begin{bmatrix} \sqrt{2}\Re\mathbf{X}_{\mathfrak{C}^+} & \mathbf{X}^{[1]}_{\mathfrak{T}^+} & \sqrt{2}\Im\mathbf{X}_{\mathfrak{C}^+} & \mathbf{X}^{[1]}_{\mathfrak{T}^+} \end{bmatrix} && \text{(3.13a)} \\
\mathbf{X}^{[1]}_{\mathfrak{T}^+} &= \begin{bmatrix} \mathbf{X}_{C_a^+} & \mathbf{X}_{C_b^+} & -\Im\mathbf{X}_{C_c^+} & \mathbf{X}_{C_d^+} & -\Im\mathbf{X}_{C_e^+} & \mathbf{X}_{C_f^+} \end{bmatrix} && \text{(3.13b)} \\
\mathbf{X}^{[1]}_{\mathfrak{T}^+} &= \begin{bmatrix} -\Im\mathbf{X}_{C_a^-} & \mathbf{X}_{C_b^-} & -\Im\mathbf{X}_{C_c^-} & \mathbf{X}_{C_d^-} & -\Im\mathbf{X}_{C_e^-} & -\Im\mathbf{X}_{C_f^-} \end{bmatrix} && \text{(3.13c)}
\end{aligned}$$

This can be extended further to $\mathbf{F}$ and $\mathbf{\Gamma}$. Expanding these matrix products can, and does, give us the values of the diagonalized matrices directly. An algorithm using simplified results obtained from expanding the matrix products is provided in Appendix B. As one may observe, complex arithmetic is not used. In fact, the algorithm reveals that complex calculations are not necessary at all for derivation of the SPEs, and one may simply store the real and imaginary parts of the complex values involved individually without being inconvenienced about complex calculations.

3.3 An Example

For an example of decoupling from this procedure, we shall make use of a system with an eigenvalue equal to zero, since both Chu and Buono (2008a) and Garvey et al. (2002a) present examples where no eigenvalues are zero. The system matrices are:

$$\mathbf{M} = \begin{bmatrix} 0.7621 & 0.4447 & 0.7382 & 0.9169 \\ 0.4565 & 0.6154 & 0.1763 & 0.4103 \\ 0.0185 & 0.7919 & 0.4057 & 0.8936 \\ 0.8214 & 0.9218 & 0.9355 & 0.0579 \end{bmatrix} \tag{3.14}$$

$$\mathbf{K} = \begin{bmatrix} 0.2111 & -0.6014 & -0.48997 & 1.2366 \\ 1.1902 & 0.5512 & 0.44908 & -0.6313 \\ -1.1162 & -1.0998 & -0.89603 & -2.3252 \\ 0.6353 & 0.086 & 0.070066 & -1.2316 \end{bmatrix} \tag{3.15}$$

$$\mathbf{C} = \begin{bmatrix} 0.371 & -1.0226 & 0.3155 & 0.5045 \\ 0.7283 & 1.0378 & 1.5532 & 1.8645 \\ 2.1122 & -0.3898 & 0.7079 & -0.3398 \\ -1.3573 & -1.3813 & 1.9574 & -1.1398 \end{bmatrix} \tag{3.16}$$

[1]Refer Appendix A for an explanation of the subscripts.

Here, $\mathbf{K}$ is singular. Hence eigenvalues would be zero. As the nullity of $\mathbf{K}$ is 1, only one eigenvalue should be zero, and this is indeed the case. The eigenvalues (sorted by absolute value) are:

$$\left\{0, \quad -0.13669 \pm 0.47519\iota, \quad -1.7264 \pm 0.36492\iota, \quad 0.087312 \pm 2.4286\iota, \quad 3.4173\right\} \tag{3.17}$$

The SPEs are:

$$\mathbf{\Pi}_L = \begin{bmatrix} -4.3438 & -9.3035 & 0.9329 & 3.8414 & 0.64854 & 2.3448 & 1.8965 & -1.3706 \\ -4.0555 & -3.2867 & 0.38837 & 2.0024 & 5.956 & 4.4991 & -0.61423 & -2.7666 \\ -38.405 & 67.603 & 7.7113 & -2.1625 & -14.964 & 21.717 & -70.529 & -49.728 \\ -0.071343 & -0.43711 & 0.77466 & -0.043924 & -0.2438 & -1.4938 & 2.6473 & -0.1501 \\ -2.6527 & -9.5906 & -7.7571 & 5.606 & -3.6186 & -6.6816 & 3.0535 & 2.3088 \\ -1.9128 & -1.4449 & 0.19726 & 0.88851 & 2.5491 & 1.7025 & -0.29276 & -1.0655 \\ 2.5338 & -3.6772 & 11.942 & 8.42 & -37.963 & 66.961 & 9.7967 & -0.69221 \\ 0 & 0 & 0 & 0 & 0 & 0 & 0 & 0 \end{bmatrix} \tag{3.18}$$

$$\mathbf{\Pi}_R = \begin{bmatrix} 7.4028 & -0.08227 & -0.32704 & -0.1583 & -10.226 & -0.059461 & 1.1118 & 0 \\ -7.626 & 0.074557 & -14.944 & 0.015977 & 15.84 & 0.080423 & 1.4468 & 0 \\ 8.9447 & 0.32858 & 6.8018 & 0.06258 & 16.439 & 0.28605 & 3.5329 & 0 \\ -0.68185 & -0.28094 & 4.5378 & 0.071865 & 2.6872 & -0.21892 & -1.7018 & 0 \\ 2.5002 & 0.18514 & -6.5661 & -0.54095 & 10.198 & 0.12304 & -0.1329 & 0 \\ -3.8727 & -0.25042 & -8.5445 & 0.054599 & -11.956 & -0.20313 & -14.691 & 0 \\ -4.0191 & -0.89067 & -20.865 & 0.21386 & 4.4507 & -0.65909 & 7.4188 & 0 \\ -0.65698 & 0.68167 & 10.051 & 0.24559 & -1.4164 & 0.47497 & 4.2406 & 0 \end{bmatrix} \tag{3.19}$$

Obviously, both SPEs are singular, but a column or row of zeros need not be present for all such cases. And the diagonalized matrices:

$$\mathbf{M}_D = diag\begin{bmatrix} 201.74 & 0.16746 & 524.19 & 0 \end{bmatrix} \tag{3.20}$$

$$\mathbf{K}_D = diag\begin{bmatrix} 49.323 & 0.52144 & 3095.8 & 1 \end{bmatrix} \tag{3.21}$$

$$\mathbf{C}_D = diag\begin{bmatrix} 55.151 & 0.57823 & -91.537 & -0.29263 \end{bmatrix} \tag{3.22}$$

The corresponding quadratic eigenvalue equations are:

$$201.74\lambda^2 + 55.151\lambda + 49.323 = 0 \Rightarrow \lambda = -0.13669 \pm 0.47519\iota \tag{3.23}$$

$$0.16746\lambda^2 + 0.57823\lambda + 0.52144 = 0 \Rightarrow \lambda = -1.7265 \pm 0.3649\iota \tag{3.24}$$

$$524.19\lambda^2 - 91.537\lambda + 3095.8 = 0 \Rightarrow \lambda = 0.087312 \pm 2.4286\iota \tag{3.25}$$

As we can see, a diagonal element of $\mathbf{M}_D$ is 0, and the corresponding (linear) polynomial $0.29263\lambda - 1 = 0$ has the solution $\lambda = 3.4173$, the only other real eigenvalue.

3.4 An Alternate Formulation

As we have seen, an eigenvalue being zero results in a singular diagonalized mass matrix. Since the transformation is done in a $2n \times 2n$ matrix space, this mass matrix doesn't correspond to a physical mass, but rather to a amalgam of the system properties. While the singularity of the mass matrix does not pose a computational problem so far, this oddity might have consequences not yet known. Consider the original LAMs, presented again for convenience:

$$\mathbf{A} = \begin{bmatrix} -\mathbf{K} & \mathbf{0} \\ \mathbf{0} & \mathbf{M} \end{bmatrix} \tag{3.26}$$

$$\mathbf{B} = \begin{bmatrix} \mathbf{C} & \mathbf{M} \\ \mathbf{M} & \mathbf{0} \end{bmatrix} \tag{3.27}$$

$$L(\lambda) := \mathbf{B}\lambda - \mathbf{A} = 0 \tag{3.28}$$

As seen in the example above, the transformation matrices are also singular – in fact, they have respectively a column and a row entirely zero. Since the common matrix to both LAMs is $\mathbf{M}$, and further the column and row which are zero are located such that both affect $\mathbf{M}$. If the common matrix were changed to another, with a corresponding change in location of zero-valued column and row, then we might be able to avoid a singular $\mathbf{M}_D$. As mentioned in section 2.2, there are three LAMs, any two of which can be used to linearise the quadratic eigenvalue problem. So far we have used only one pair. We theorized that by using alternate LAMs, we may be able to avoid singular mass matrices. To this end, consider the LAM $\mathbf{D}$:

$$\mathbf{D} = \begin{bmatrix} 0 & \mathbf{K} \\ \mathbf{K} & \mathbf{C} \end{bmatrix} \tag{3.29}$$

paired with $\mathbf{A}$ to obtain the corresponding eigenvalue problem:

$$L(\lambda) := \lambda\mathbf{A} + \mathbf{D} = 0 \tag{3.30}$$

For this matrix pencil, the transformation matrices are different, as is the construction of the intermediate matrices. The intermediate matrices, where different, are presented here:

$$\mathbf{P} = \mathbf{I}_{2n} \left[\mathfrak{C}^{-} \mathfrak{T}^{-} \mathfrak{T}^{+} \mathfrak{C}^{+} \right] \tag{3.31a}$$

$$\mathbf{J}_L = \begin{bmatrix} \mathbf{L}^{-} & \mathbf{0} & \mathbf{0} & \mathbf{0} \\ \mathbf{0} & \frac{-\iota}{\sqrt{2}}\mathbf{I}_p & \mathbf{0} & \frac{1}{\sqrt{2}}\mathbf{I}_p \\ \mathbf{0} & \mathbf{0} & \mathbf{L}^{+} & \mathbf{0} \\ \mathbf{0} & \frac{\iota}{\sqrt{2}}\mathbf{I}_p & \mathbf{0} & \frac{1}{\sqrt{2}}\mathbf{I}_p \end{bmatrix} \tag{3.31b}$$

$$\mathbf{J}_R = \begin{bmatrix} \mathbf{R}^{-} & \mathbf{0} & \mathbf{0} & \mathbf{0} \\ \mathbf{0} & \frac{-\iota}{\sqrt{2}}\mathbf{I}_p & \mathbf{0} & \frac{1}{\sqrt{2}}\mathbf{I}_p \\ \mathbf{0} & \mathbf{0} & \mathbf{R}^{+} & \mathbf{0} \\ \mathbf{0} & \frac{\iota}{\sqrt{2}}\mathbf{I}_p & \mathbf{0} & \frac{1}{\sqrt{2}}\mathbf{I}_p \end{bmatrix} \tag{3.31c}$$

$$\mathbf{F} = \begin{bmatrix} \mathbf{\Psi}^{-} & \mathbf{0} & \mathbf{I}_{n-p} & \mathbf{0} \\ \mathbf{0} & \mathbf{\Phi} & \mathbf{0} & \mathbf{I}_{p} \\ \mathbf{I}_{n-p} & \mathbf{0} & \mathbf{\Psi}^{+} & \mathbf{0} \\ \mathbf{0} & \mathbf{I}_{p} & \mathbf{0} & \mathbf{\Phi} \end{bmatrix} \tag{3.31d}$$

$$\mathbf{\Theta} = \mathbf{A}_{11}^{-1}\mathbf{D}_{12} \tag{3.31e}$$

When $\mathbf{A}$ and $\mathbf{B}$ were used, if $\mathbf{M}$ or $\mathbf{K}$ were singular, then some eigenvalues would be zero. Unfortunately, when $\mathbf{A}$ and $\mathbf{D}$ are used, the corresponding eigenvalues are infinite. While a workaround existed for the earlier approach, whereby pseudo-inverses where used instead of inverses, no such workaround could be obtained for this alternate approach. However, some computations are eliminated (see Appendix A for details). So, for large non-singular systems, the LAMs should be $\mathbf{A}$ and $\mathbf{D}$, but for singular systems, the LAMs should be $\mathbf{A}$ and $\mathbf{B}$. The expanded vector-based algorithm presented in Appendix B is not repeated for the alternate approach, since it is trivial to obtain the required changes from the changes in the intermediate matrices. A similar situation holds true for the third pair of LAMs, $\mathbf{B}$ and $\mathbf{D}$. Again, eigenvalues become infinite instead if the component matrices are zero. Since there seemed to be no advantage here, the intermediate matrices were not derived.

3.5 Stable Filters

So far, we have been discussing decoupling transformations, which are generally in the $\mathbb{R}^{2n\times 2n}$ space. Since the control systems will operate in the $\mathbb{R}^{n\times n}$ space, we must derive appropriate filters from the decoupling transformations. These filters will be used whenever we exert control, so that their stability is of paramount importance. To this end, we shall use Automorphic Transformations which map a matrix to itself, which we can select based upon our stability criteria to obtain appropriate filters. However, the mapping is of the form $f(\theta^n) : \mathbb{R}^n \to \mathbb{R}^{2n\times 2n}$, and thus far the exact nature of the mapping has not been established. Therefore we must rely on either (a) exhaustive tables of results, which quickly become unwieldy in practice, or (b) a Monte Carlo search for an appropriate filter. The notion of filter goodness described in Jiffri (2011) shall be our criteria for selecting filters. We shall discuss both these methods in the next two chapters.

Chapter 4

Stable Filters

In this chapter we will know the meaning and use of stable filters. By structure preserving transformation we get diagonalized LAMs but it doesn't solve our generalized equation of motion problem, just to remind, we are trying to find out decoupled equation of motion of any dynamic system. With SPE, we got diagonalized LAMs using special transformation matrix as described in previous chapters, now here we will learn what additional steps are required to convert our generalized coupled equation of motion into decoupled form in order to easily solve it. As can be seen from Figure 4.1 below, it is the modal filters that are used in the actual control system. Hence, their stability with respect to their eigenvalues is of paramount importance when it comes to designing the controller.

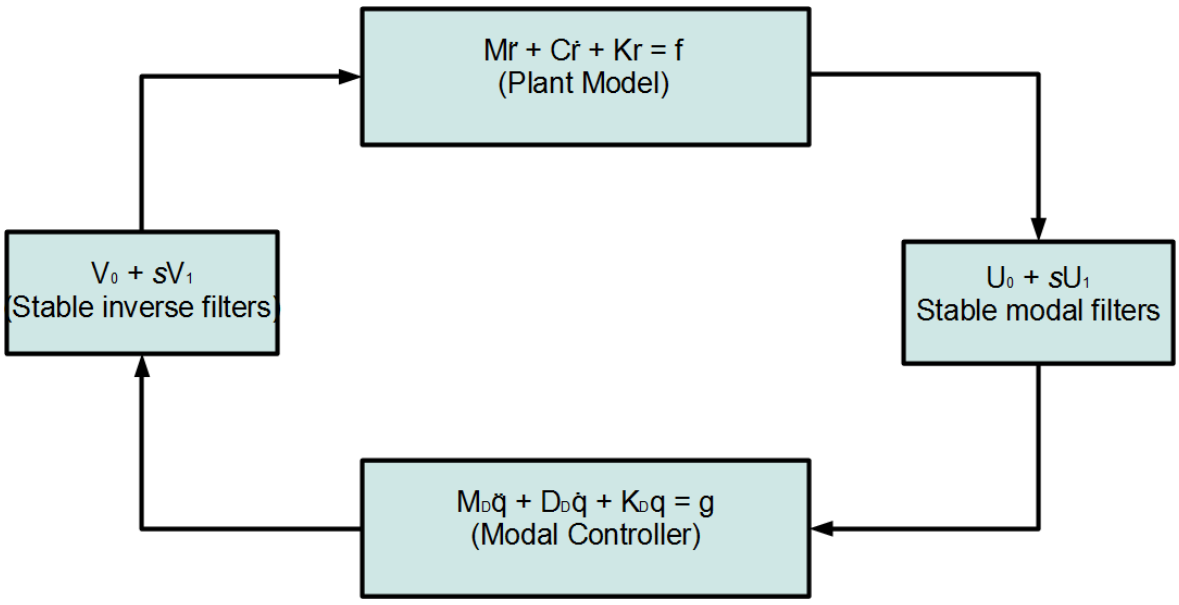

Figure 4.1: Modal Controller with diagonalizing filters

4.1 Definition and Necessity of Stable Filters

Any dynamic system can be expressed by *lumped parameters* as:

$$\begin{bmatrix} \mathbf{0} & \mathbf{K}_0 \\ \mathbf{K}_0 & \mathbf{C}_0 \end{bmatrix} \begin{bmatrix} \mathbf{q} \\ \dot{\mathbf{q}} \end{bmatrix} - \begin{bmatrix} \mathbf{K}_0 & 0 \\ 0 & -\mathbf{M}_0 \end{bmatrix} \begin{bmatrix} \dot{\mathbf{q}} \\ \ddot{\mathbf{q}} \end{bmatrix} = \begin{bmatrix} \mathbf{0} \\ \mathbf{f} \end{bmatrix} \tag{4.1}$$

The Laplace transform of this equation gives:

$$\left\{ \begin{bmatrix} \mathbf{0} & \mathbf{K}_0 \\ \mathbf{K}_0 & \mathbf{C}_0 \end{bmatrix} - s \begin{bmatrix} \mathbf{K}_0 & \mathbf{0} \\ \mathbf{0} & -\mathbf{M}_0 \end{bmatrix} \right\} \begin{bmatrix} \underline{\mathbf{q}} \\ \underline{\mathbf{q}}s \end{bmatrix} = \begin{bmatrix} \mathbf{0} \\ \underline{\mathbf{f}} \end{bmatrix} \tag{4.2}$$

Or

$$\left\{ \begin{bmatrix} \mathbf{K}_0 & \mathbf{0} \\ \mathbf{0} & -\mathbf{M}_0 \end{bmatrix} - s \begin{bmatrix} -\mathbf{C}_0 & -\mathbf{M}_0 \\ -\mathbf{M}_0 & \mathbf{0} \end{bmatrix} \right\} \begin{bmatrix} \underline{\mathbf{q}} \\ \underline{\mathbf{q}}s \end{bmatrix} = \begin{bmatrix} \underline{\mathbf{f}} \\ \mathbf{0} \end{bmatrix} \tag{4.3}$$

We define the following:

$$\begin{bmatrix} \mathbf{u} \\ \mathbf{v} \end{bmatrix} = \begin{bmatrix} \mathbf{P}_R & \mathbf{Q}_R \\ \mathbf{R}_R & \mathbf{S}_R \end{bmatrix} \begin{bmatrix} \underline{\mathbf{q}} \\ \underline{\mathbf{q}}s \end{bmatrix} \tag{4.4}$$

or

$$\begin{bmatrix} \underline{\mathbf{q}} \\ \underline{\mathbf{q}}s \end{bmatrix} = \begin{bmatrix} \mathbf{W}_R & \mathbf{X}_R \\ \mathbf{Y}_R & \mathbf{Z}_R \end{bmatrix} \begin{bmatrix} \mathbf{u} \\ \mathbf{v} \end{bmatrix} \tag{4.5}$$

more,

$$\begin{bmatrix} \mathbf{d} \\ \mathbf{e} \end{bmatrix} = \begin{bmatrix} \mathbf{W}_L & \mathbf{X}_L \\ \mathbf{Y}_L & \mathbf{Z}_L \end{bmatrix}^T \begin{bmatrix} \mathbf{0} \\ \underline{\mathbf{f}} \end{bmatrix} \tag{4.6}$$

and

$$\begin{bmatrix} \mathbf{h} \\ \mathbf{j} \end{bmatrix} = \begin{bmatrix} \mathbf{W}_L & \mathbf{X}_L \\ \mathbf{Y}_L & \mathbf{Z}_L \end{bmatrix}^T \begin{bmatrix} \underline{\mathbf{f}} \\ \mathbf{0} \end{bmatrix} \tag{4.7}$$

where $\mathbf{W}_R$ etc. are obtained from transformation, now when we apply these conditions on our equation system obtained after Laplace transform, we get,

$$\left\{ \begin{bmatrix} \mathbf{K}_D & \mathbf{0} \\ \mathbf{0} & -\mathbf{M}_D \end{bmatrix} - s \begin{bmatrix} -\mathbf{C}_D & -\mathbf{M}_D \\ -\mathbf{M}_D & \mathbf{0} \end{bmatrix} \right\} \begin{bmatrix} \mathbf{u} \\ \mathbf{v} \end{bmatrix} = \begin{bmatrix} \mathbf{h} \\ \mathbf{j} \end{bmatrix} \tag{4.8}$$

Premulptiplying this equation with

$$\begin{bmatrix} \mathbf{I} & s\mathbf{I} \end{bmatrix} \tag{4.9}$$

we get,

$$\begin{bmatrix} \mathbf{K}_D & -s\mathbf{M}_D \end{bmatrix} \begin{bmatrix} \mathbf{u} \\ \mathbf{v} \end{bmatrix} + \begin{bmatrix} s\mathbf{C}_D + s^2\mathbf{M}_D & s\mathbf{M}_D \end{bmatrix} \begin{bmatrix} \mathbf{u} \\ \mathbf{v} \end{bmatrix} = [\mathbf{h} + s\mathbf{j}] \tag{4.10}$$

which gives;

$$\mathbf{K}_D\mathbf{u} + s\mathbf{C}_D\mathbf{u} + s^2\mathbf{M}_D\mathbf{u} = \mathbf{h} + s\mathbf{j} \tag{4.11}$$

But since;

$$\begin{bmatrix} \mathbf{h} \\ \mathbf{j} \end{bmatrix} = \begin{bmatrix} \mathbf{W}_L & \mathbf{X}_L \\ \mathbf{Y}_L & \mathbf{Z}_L \end{bmatrix}^T \begin{bmatrix} \underline{\mathbf{f}} \\ \mathbf{0} \end{bmatrix} \tag{4.12}$$

hence,

$$\begin{bmatrix} \mathbf{I} & s\mathbf{I} \end{bmatrix} \begin{bmatrix} \mathbf{h} \\ \mathbf{j} \end{bmatrix} = \begin{bmatrix} \mathbf{I} & s\mathbf{I} \end{bmatrix} \begin{bmatrix} \mathbf{W}_L & \mathbf{X}_L \\ \mathbf{Y}_L & \mathbf{Z}_L \end{bmatrix}^T \begin{bmatrix} \underline{\mathbf{f}} \\ \mathbf{0} \end{bmatrix} \tag{4.13}$$

which gives

$$\mathbf{h} + s\mathbf{j} = ({\mathbf{W}_L}^T + s{\mathbf{X}_L}^T)\underline{\mathbf{f}} \tag{4.14}$$

and hence,

$$(\mathbf{K}_D + s\mathbf{C}_D + s^2\mathbf{M}_D)(\mathbf{P}_R + s\mathbf{Q}_R)\underline{\mathbf{q}} = ({\mathbf{W}_L}^T + s{\mathbf{X}_L}^T)\underline{\mathbf{f}} \tag{4.15}$$

further more,

$$({\mathbf{W}_L}^T + s{\mathbf{X}_L}^T)^{-1}(\mathbf{K}_D + s\mathbf{C}_D + s^2\mathbf{M}_D)(\mathbf{P}_R + s\mathbf{Q}_R)\underline{\mathbf{q}} = (\mathbf{K}_0 + s\mathbf{C}_0 + s^2\mathbf{M}_0)\underline{\mathbf{q}} \tag{4.16}$$

which implies,

$$(\mathbf{K}_D + s\mathbf{C}_D + s^2\mathbf{M}_D)(\mathbf{P}_R + s\mathbf{Q}_R) = ({\mathbf{W}_L}^T + s{\mathbf{X}_L}^T)(\mathbf{K}_0 + s\mathbf{C}_0 + s^2\mathbf{M}_0) \tag{4.17}$$

assuming, $\mathbf{P}_R$ and $\mathbf{Q}_R$ are represented by $\mathbf{V}_0$ and $\mathbf{V}_1$ respectively, similarly ${\mathbf{W}_L}^T$ and ${\mathbf{X}_L}^T$ are represented by $\mathbf{U}_0$ and $\mathbf{U}_1$ respectively.Then,

$$(\mathbf{K}_D + s\mathbf{C}_D + s^2\mathbf{M}_D)(\mathbf{V}_0 + s\mathbf{V}_1) = (\mathbf{U}_0 + s\mathbf{U}_1)(\mathbf{K}_0 + s\mathbf{C}_0 + s^2\mathbf{M}_0) \tag{4.18}$$

where, $(\mathbf{U}_0 + \mathrm{s}\mathbf{U}_1)$ and $(\mathbf{V}_0 + \mathrm{s}\mathbf{V}_1)$ are the filters, and from this proof it is clear that these filters are obtained from Structure Preserving Equivalences (SPEs), which are not unique. Since we need to find stable filters, we must check whether the poles of obtained filters are stable or not.

4.1.1 Automorphic SPE

Our four $n \times n$ matrices $\mathbf{P}_L, \mathbf{Q}_L, \mathbf{R}_L, \mathbf{S}_L$ can be expressed by two independent $n \times n$ matrices $\mathbf{F}_L, \mathbf{G}_L$, as there is dependencies among blocks of transformation matrix. the representation can be expressed as follows:

$$\begin{bmatrix} \mathbf{P}_L & \mathbf{Q}_L \\ \mathbf{R}_L & \mathbf{S}_L \end{bmatrix} = \begin{bmatrix} (\mathbf{F}_L - \frac{1}{2}\mathbf{G}_L\mathbf{C}_D) & -\mathbf{G}_L\mathbf{M}_D \\ \mathbf{G}_L\mathbf{K}_D & (\mathbf{F}_L + \frac{1}{2}\mathbf{G}_L\mathbf{C}_D) \end{bmatrix} \tag{4.19}$$

From symmetry one can also show that they can also be written by two independent matrices $\mathbf{F}_R$ and $\mathbf{G}_R$ as follows,

$$\begin{bmatrix} \mathbf{P}_R & \mathbf{Q}_R \\ \mathbf{R}_R & \mathbf{S}_R \end{bmatrix}^{-1} = \begin{bmatrix} (\mathbf{F}_R - \frac{1}{2}\mathbf{G}_R\mathbf{C}_D) & -\mathbf{G}_R\mathbf{M}_D \\ \mathbf{G}_R\mathbf{K}_D & (\mathbf{F}_R + \frac{1}{2}\mathbf{G}_R\mathbf{C}_D) \end{bmatrix} \tag{4.20}$$

These matrices must obey following law to generate a valid SPE,

$$\mathbf{F}_L{\mathbf{G}_R}^T + \mathbf{G}_L{\mathbf{F}_R}^T = \mathbf{0} \tag{4.21}$$

Now let us show this for single DOF system, than the three relations will generate following equations,

$$\begin{bmatrix} (f + \frac{1}{2}gd) & gm \\ -gk & (f - \frac{1}{2}gd) \end{bmatrix}^T \begin{bmatrix} 0 & k \\ k & d \end{bmatrix} \begin{bmatrix} (f - \frac{1}{2}gd) & -gm \\ gk & (f + \frac{1}{2}gd) \end{bmatrix} = \begin{bmatrix} 0 & k \\ k & d \end{bmatrix} \tag{4.22}$$

$$\begin{bmatrix} (f + \frac{1}{2}gd) & gm \\ -gk & (f - \frac{1}{2}gd) \end{bmatrix}^T \begin{bmatrix} k & 0 \\ 0 & -m \end{bmatrix} \begin{bmatrix} (f - \frac{1}{2}gd) & -gm \\ gk & (f + \frac{1}{2}gd) \end{bmatrix} = \begin{bmatrix} k & 0 \\ 0 & -m \end{bmatrix} \tag{4.23}$$

$$\begin{bmatrix} (f + \frac{1}{2}gd) & gm \\ -gk & (f - \frac{1}{2}gd) \end{bmatrix}^T \begin{bmatrix} d & m \\ m & 0 \end{bmatrix} \begin{bmatrix} (f - \frac{1}{2}gd) & -gm \\ gk & (f + \frac{1}{2}gd) \end{bmatrix} = \begin{bmatrix} d & m \\ m & 0 \end{bmatrix} \tag{4.24}$$

where m, k and d are mass, stiffness and damping of single DOF system, now in above equations f, represents $\mathbf{F}_L$ and $\mathbf{F}_R$ both and similarly, g, represents $\mathbf{G}_L$ and $\mathbf{G}_R$. Now g and f for multi-DOF system can be found using following equations,

$$\begin{bmatrix} (f + \frac{1}{2}gd) & gm \\ -gk & (f - \frac{1}{2}gd) \end{bmatrix} \begin{bmatrix} (f - \frac{1}{2}gd) & -gm \\ gk & (f + \frac{1}{2}gd) \end{bmatrix} = \begin{bmatrix} 1 & 0 \\ 0 & 1 \end{bmatrix} \tag{4.25}$$

which can be expressed as,

$$f^2 + g^2(km + \frac{1}{4}d^2) = 1 \tag{4.26}$$

from here it is clear that by considering these equations we are discarding one independent dimension, now we have only one independent dimension out of two., if $d^2 - 4km = 0$ then that dimension is also discarded, but if $d^2 - 4km > 0$, we can write f as multiple of $\cosh\theta$ and g can be represented by multiple of $\cosh\theta$, similarly if $d^2 - 4km < 0$, we can write f as multiple of $\cos\theta$ and g as a multiple of $\sin\theta$, which leaves us with only one independent variable θ, So now, we are capable of finding the value of $\mathbf{F}_L$ and $\mathbf{G}_L$, which will generate our stable filters by modifying SPE to convert them automorphic form. This implies that our general quadratic pencil is totally decoupled after using stable filters, so we can use any method such as ODE45 etc. to solve these decoupled equations for every DOF.

4.2 The Space of Stable Filters

In the previous section, we saw that, for each decoupled equation, the automorphic SPEs had a corresponding parameter θ. Thus, for system with $n \times n$ matrices, there would be n parameters, creating a mapping from $\mathbf{R}^n$ to $\mathbf{R}^{2n \times 2n}$. For convenience, if the system has n such parameters, we shall call it an n dimensional system. Jiffri (2011) has attempted to study this mapping, and to derive stable regions, examining 2-dimensional systems. We have attempted to replicate the results presented therein, and to extend the procedure to 3 dimensional systems. Before we proceed, let us first examine the criteria for an acceptable filter. Stability is not the only concern, hence Jiffri (2011) has proposed that an enhanced criterion, the *goodness* of a filter be considered instead.

4.2.1 Goodness of Filters

A property of the modal filters that becomes important is that the filter itself contributes to the dynamics of the overall closed-loop system. Therefore it is a prerequisite that the filters are stable (Garvey, 2008), should they operate indefinitely. This is the first property that is required of the filter. However, stability is not the only issue of concern. Another consideration that becomes important at a practical level is the magnitude of the eigenvalues of the filter. It is undesirable to use filters with eigenvalues of unnecessarily large magnitudes, as this would require that the controller has an equally high update rate raising the overall cost of the controller unit - to accommodate the high natural frequencies of the filter. This gives rise to the second property required of the filter, which is the limitation of the magnitudes of its eigenvalues. Since the update rate of the controller will necessarily be adequate to accommodate the closed-loop system eigenvalue with the largest magnitude, a filter is desired such that its largest eigenvalue is smaller than or equal to the largest eigenvalue of the dynamic system. Thus, the desirable maximum allowable eigenvalue magnitude for the filter may be set on this basis.

Using the above two criteria, one defines the notion of filter goodness. Since filters are non-unique, it is possible to find some filters that are better than others, with the use of automorphic transformations. Filters that conform to this notion of goodness will have their eigenvalues located within a certain desirable envelope.

Eigenvalues and Characteristic Polynomials of Filters

We have not considered the characteristic polynomial of the system till now. But now, the coefficients of the characteristic polynomial (in monic form) will be of essence to the discussion hereafter. So, let us have a brief overview of the polynomial and its coefficients.

For an n dimensional system, the characteristic polynomial in monic form is:

$$P(\lambda) = \lambda^n + p_1\lambda^{n-1} + \ldots + p_n \tag{4.27}$$

Now, there are n coefficients $p_1, \ldots, p_n$, all necessarily real, since the filters themselves are real-valued. These coefficients are called the Characteristic Polynomial Coefficients

(CPCs). The eigenvalues may or may not be real. But, since we are concerned with the eigenvalues, and not the exact filter itself, pairs of filters with the same eigenvalues (and hence the same CPCs) are equivalent. Therefore, we need concern ourselves only with the Characteristic Polynomial Coefficients (CPCs) of the filters. Then the original mapping, $f(\mathbf{\Theta}) : \mathbb{R}^n \to \mathbb{R}^{2n\times 2n}$, can be reduced to $g(\mathbf{\Theta}) : \mathbb{R}^n \to \mathbb{R}^n$. Furthermore, the CPCs are especially convenient when it comes to visualising the mapping, in the 2 and 3 dimensional cases. The eigenvalues are not well suited for this purpose, since they, while being of equal number, may or may not have two components, depending upon the complex nature of the eigenvalues. In the 2 dimensional case, of course, this is not a problem. Indeed, plotting the eigenvalues in the complex plane does prove interesting.

4.3 Examples

4.3.1 Stable Filters for a 3-dimensional system

For the 3 dimensional case, the system matrices used (Garvey, 2008) and initial filters are:

$$\mathbf{M} = \mathbf{I}_3, \quad \mathbf{C} = \begin{bmatrix} 0 & 7 & -8 \\ -7 & 0 & 10 \\ 8 & -10 & 0 \end{bmatrix}, \quad \mathbf{K} = \begin{bmatrix} 600 & -100 & 10 \\ -100 & 400 & 10 \\ 10 & 100 & 200 \end{bmatrix} \tag{4.28}$$

$$\mathbf{U}_0 = \begin{bmatrix} -18.921 & 8.1454 & 24.379 \\ 21.205 & 31.517 & 5.9355 \\ 45.665 & -31.915 & 6.199 \end{bmatrix}, \mathbf{U}_1 = \begin{bmatrix} -0.01043 & 0.98809 & -0.90536 \\ 1.2074 & 0.7416 & 1.003 \\ 2.2827 & -0.48804 & -1.5629 \end{bmatrix} \tag{4.29}$$

$$\mathbf{V}_0 = \begin{bmatrix} -0.036901 & -0.020032 & 0.12456 \\ 0.049178 & 0.085341 & 0.022948 \\ 0.063627 & -0.071727 & 0.031398 \end{bmatrix}, \mathbf{V}_1 = \begin{bmatrix} -8.1156e-05 & 0.0076881 & -0.0070443 \\ 0.003052 & 0.0018746 & 0.0025354 \\ 0.0025605 & -0.00054745 & -0.0017531 \end{bmatrix} \tag{4.30}$$

The eigenvalues of the initial filters are $26.93, 22.888$ and -15.107. The filter eigenvalues are all real, whereas the system eigenvalues are all complex: $-0.43177 \pm 29.854\iota, -0.4482 \pm 19.883\iota$ and $0.88019 \pm 11.294\iota$. So, while the greatest filter eigenvalue is less than the greatest absolute value of the system eigenvalues (26.93 and 29.857, respectively), the filter eigenvalues are not stable. We now examine the space of filters to obtain stable, good filters.

Now, the range of $\mathbf{\Theta}$ is taken to be $[0, \pi]\times[0, \pi]\times[0, \pi]$ (Jiffri, 2011, App. C). Discretizing this rage uniformly into $100\times100\times100$ points, we proceed to check each point. The criteria for a good filter is: a) The greatest filter eigenvalue should be less than the greatest system eigenvalue; and b) All eigenvalues must have a negative real part. One set of good filters,

corresponding to $\mathbf{\Theta} = (0, 0.12693, 0.15867)$, are:

$$\mathbf{U}_0^{=} \begin{bmatrix} 11.579 & -27.706 & 13.267 \\ -7.6859 & 13.349 & -3.3902 \\ 13.199 & -16.51 & 10.612 \end{bmatrix}, \mathbf{U}_1^{=} \begin{bmatrix} -0.42074 & -0.15095 & 1.3469 \\ 1.5284 & 1.705 & 1.0209 \\ 2.9306 & -1.5688 & -0.79121 \end{bmatrix} \tag{4.31}$$

$$\mathbf{V}_0^{=} \begin{bmatrix} 0.003798 & -0.085795 & 0.070334 \\ -0.006439 & 0.036371 & -0.018446 \\ 0.012426 & -0.051926 & 0.055033 \end{bmatrix}, \mathbf{V}_1^{=} \begin{bmatrix} -0.0032737 & -0.0011745 & 0.01048 \\ 0.0038636 & 0.0043099 & 0.0025806 \\ 0.0032873 & -0.0017598 & -0.00088752 \end{bmatrix} \tag{4.32}$$

This set of filters have eigenvalues $-0.54937 \pm 1.3887\iota$ and -28.576, which satisfy both our criteria. Note that the eigenvalues of the pair $(\mathbf{U}_0, -\mathbf{U}_1)$ are the same as those of $(\mathbf{V}_0, -\mathbf{V}_1)$, and the automorphic transforms affect both pairs equally. So we shall not explicitly state one pair, $(\mathbf{V}_0, -\mathbf{V}_1)$, from now on.

4.3.2 Stable Filters for a 2-dimensional system

For the 2 dimensional case, the system matrices used, along with the corresponding left and right filters, are:

$$\mathbf{M} = \begin{bmatrix} 1 & 0 \\ 0 & 1 \end{bmatrix}, \quad \mathbf{C} = \begin{bmatrix} 0 & -1 \\ -1 & 0 \end{bmatrix}, \quad \mathbf{K} = \begin{bmatrix} 75 & 0 \\ 0 & 1 \end{bmatrix} \tag{4.33}$$

$$\mathbf{U}_0 = \begin{bmatrix} -0.51564 & -0.50522 \\ -12.789 & -0.020095 \end{bmatrix}, \qquad \mathbf{U}_1 = \begin{bmatrix} -0.0069222 & 0.50867 \\ -1.4667 & 0.17285 \end{bmatrix} \tag{4.34}$$

The eigenvalues of the filter pairs are real: -8.6234 and 1.0043, whereas the eigenvalues of the system are all purely imaginary: $\pm 8.6015\iota$ and $\pm 1.0068\iota$. Since one filter eigenvalue is positive (and therefore unstable), and they just exceed the eigenvalues of the system, they are not good enough. We now examine the space of filters to obtain stable, good filters.

The range of $\mathbf{\Theta}$ is taken to be $[0, \pi] \times [0, \pi]$, discretized uniformly in to 625×625 points. In addition to the criteria used in the previous example, for limiting the area of the graph, all CPCs should be less than a specific value (here, arbitrarily taken to be 100). This last limitation is not of great import, since once the area of good filters is obtained (as can be seen on the plot), we can remove this restriction when focusing on that particularly area. A set of stable filters for this system would be:

$$\mathbf{U}_0^{=} \begin{bmatrix} 0.7242 & -0.078479 \\ 10.307 & 0.023353 \end{bmatrix}, \qquad \mathbf{U}_1^{=} \begin{bmatrix} -0.0010753 & -0.71502 \\ 1.7044 & -0.13931 \end{bmatrix} \tag{4.35}$$

These filters correspond to $\mathbf{\Theta} = (0.89252, 1.7215)$, and have eigenvalues -5.9597, -0.11369. The filter eigenvalues now match our goodness criteria very well.

4.4 Unreachable Regions for Automorphic Transforms

Before we focus on the area of good filters, let us study the area of available filters. Now, for a quadratic polynomial, the coefficients corresponding to complex roots lie within a parabola. This is easily established, since, for complex roots of a monic polynomial $P(\lambda) = \lambda^2 + x\lambda + y$, we must have $x^2 - 4y < 0$. Whether an eigenvalue is complex or not is not of much importance. But for this system of matrices, and indeed it seems for most such systems, there appear to be regions inaccessible via automorphic SPEs. And, in the 2-dimensional case, such regions seem to share two common properties:

1. They are conic sections;

2. They lie within this parabola.

For certain systems, for example the system in the previous example, the entire parabola is inaccessible. A plot of the corresponding eigenvalues reveals that these inaccessible regions have their analogues in the eigenspace. For the present system, since the entire parabola was inaccessible by automorphic transforms, eigenvalues of all stable filters are necessarily real.

These special areas also exist for the 3-dimensional case, and presumably for all dimensions. In the 3-dimensional case, contrary to what one might expect, these regions are not cones or revolutions of conic sections, but have quite arbitrary shapes, with symmetry a common feature in the cases examined so far. The high number of variables involved have made analytical derivation of the equations of these regions very difficult. One way to do it numerically would be to evaluate the Jacobian at each point. Anywhere outside the unreachable region, a point can move in any direction. However, at the surface of the region, the point is constrained from moving further within the region. Thus the derivative of the coordinate vector along these directions would be zero. Hence the Jacobian would be rank-deficient, and its determinant would be zero. This is true independent of the basis chosen for obtaining the Jacobian. Thus, but determining where the Jacobian is zero, one can approximate the surface of the unreachable region.

This method was applied to the present example. For evaluating the partial derivatives that make up the Jacobian, a first-order finite difference method was used. Then a root-finding algorithm was applied on the Jacobian determinant for each grid line. The resultant boundary points are shown in Figure 4.4. The fit (quadratic) is reasonably accurate, as can be inferred from the figure. The extra points are due to the gaps in calculated points, which arise due to the uniform intervals in which the range of values of $\mathbf{\Theta}$ was divided. The bottom edge, and some of the gaps in the space of stable points, which may or may not be unreachable, were also detected by this method.

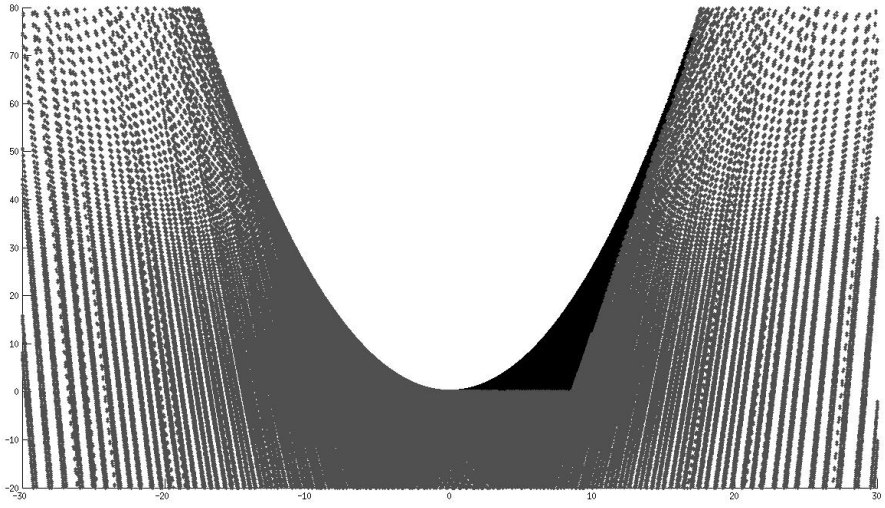

Figure 4.2: Good CPCs (shown in black) and reachable CPCs of a 2D system

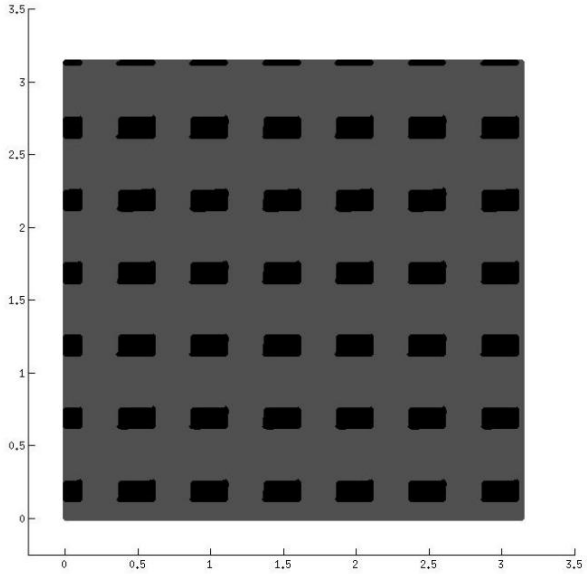

Figure 4.3: Scatter of (θ_1, θ_2) for good CPCs (in black) over reachable CPCs

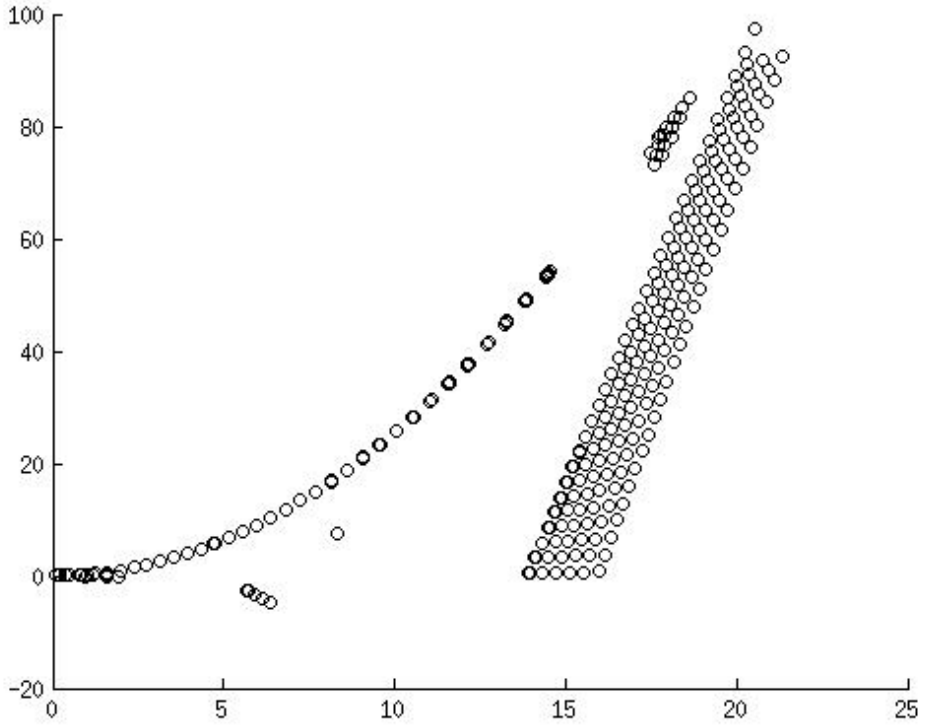

Figure 4.4: Calculated boundary points of unreachable CPC region

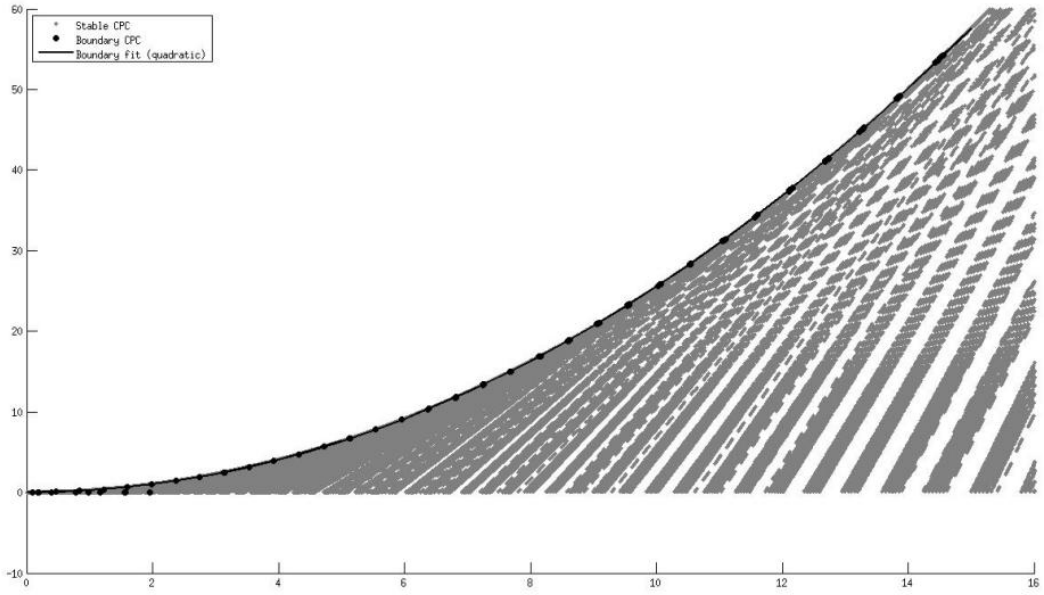

Figure 4.5: Fit of boundary points over all CPC points

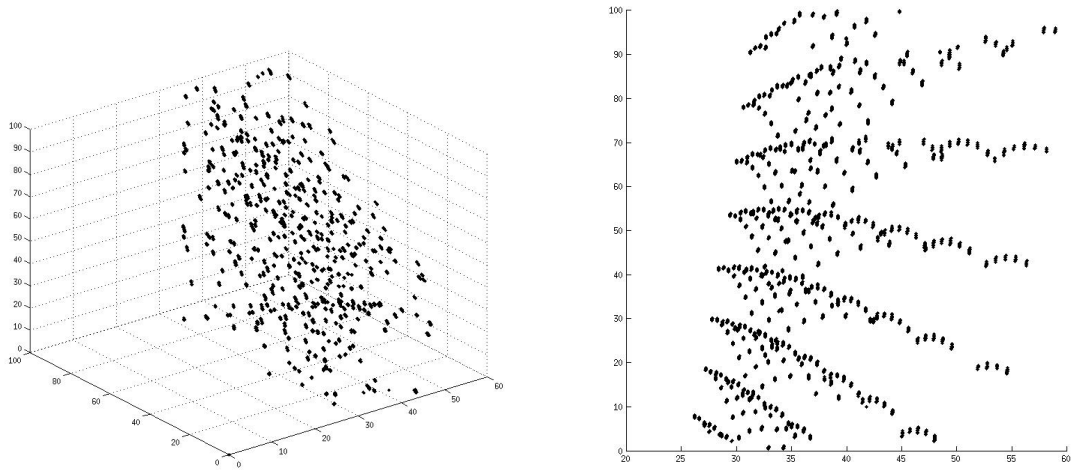

(a) A 3D scatter, seemingly random (b) Projection on the x-y plane, revealing a pattern.

Figure 4.6: Good CPCs for a 3D system

Chapter 5

Monte Carlo Search

5.1 Introduction to Monte Carlo experiments

Monte Carlo experiments are a class of computational algorithms that rely on repeated random sampling to compute their results. Monte Carlo methods are often used in computer simulations of physical and mathematical systems. These methods are most suited to calculation by a computer and tend to be used when it is infeasible to compute an exact result with a deterministic algorithm. This method is also used to complement theoretical derivations. In an Monte Carlo search, input values are drawn from some probability distribution, say the normal or the Poisson distributions. The corresponding output values are computed and compared. The distribution used may affect the quality of the results, and should be chosen carefully.

5.2 Random Searches vs. Sequential Searches

Using a fixed grid for searching the space of stable filters has its pitfalls. For one, as can be seen from the figures of the previous chapter, as one moves further away from the origin in the CPC plane, the lines move further apart. It is not easy to provide a gradient to the intervals in which the range of $\mathbf{\Theta}$ is discretized, since different systems have different spaces of stable filters. So far, in the cases studied, the area of stable filters seems to be dense around the origin, both for 2D and 3D systems. But it is difficult to predict which values of $\mathbf{\Theta}$ correspond to CPCs near the origin. Sometimes, values of $\mathbf{\Theta}$ corresponding to the points in the stable region might lie quite far from the origin, in which case sequential search would go a long while without yielding stable points, whereas an uniform distribution Monte Carlo search could chance upon stable points much sooner, as it looks at the entire grid.

Using the 2D system presented in subsection 4.3.2, a comparison of the number of stable points discovered by both sequential and Monte Carlo (uniform distribution) searches was made. The result can be seen in Figure 5.2. The Monte Carlo method provided a constant stream of stable points, where as the sequential search had bursts of rapid success followed

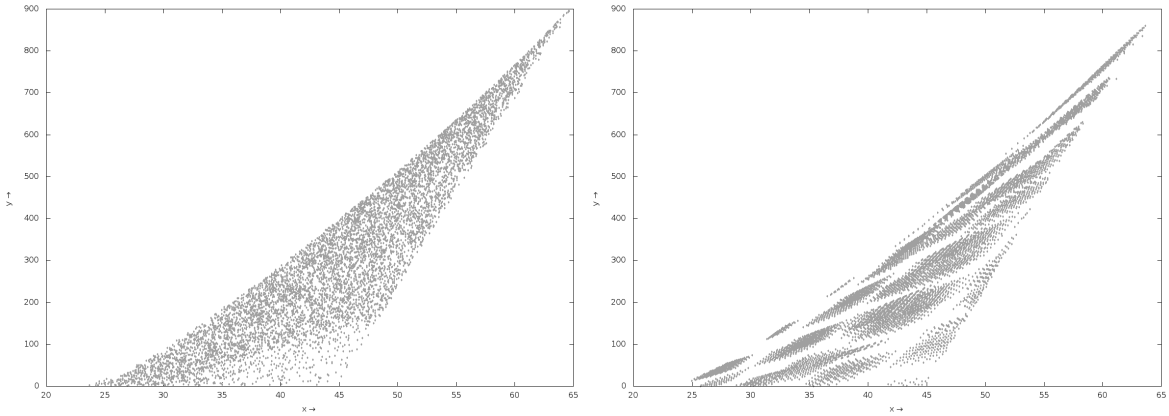

(a) Monte Carlo method

(b) Sequential search

Figure 5.1: Comparison of Stable Points returned by Monte Carlo and Sequential searches

by plateaus of stagnation. Indeed, the sequential search showed no increase in the number of stable points for around 500,000 points during each period of stagnation. Also, a number of stable points were discovered by the Monte Carlo search in the gaps left by the sequential search (while, of course, missing points found by the sequential search).

We theorize that the apparent gaps in the region of stable filters, apart from the unreachable region discussed in section 4.4, is due to the fixed, uniform discretization used in the sequential search, and the gaps apparent in (Jiffri, 2011, Fig. 4-10) would not have followed the distinctive pattern, had a Monte Carlo search been used. Indeed, a glance at Figure 5.1 will reveal that some pattern is apparent in the sequential search results, whereas nothing of the sort is visible in the results of the Monte Carlo experiment. Interestingly, a comparison of Monte Carlo searches using different distributions does not show such differences. Both uniform and normal distribution show similar performance, the normal distribution being just slower than the uniform distribution for the same 2D system. However, the regions of $\mathbf{\Theta}$ evaluated by each prove insightful. In both cases, (see Figure 4.3), the points corresponding to stable CPCs are clustered in rectangular regions around some points which are located over a repeating pattern. So a possible way to speed up the search for stable points would be to do a Monte Carlo search using the uniform distribution to obtain a small number of initial, evenly spread points, and then execute searches using the normal distribution centred over these seed points.

In fact, this does considerably speed up the search process. Depending upon how many seed points were generated, the process would accelerate sharply after a certain stage, and produce around 36,000 stable points for every 100,000 points discarded, whereas just using one distribution would only produce around 18,000 stable points per 100,000 discarded – a speed-up by a factor of 2. The stage at which this sudden increase in rate of discovery occurs can be pushed back to happen earlier by using fewer seed points. The optimum number of seed points seems to be around 10,000, with both 5000 and 20,000 points showing the speed-up at a later stage. A comparison of the rates of this Monte Carlo method (with

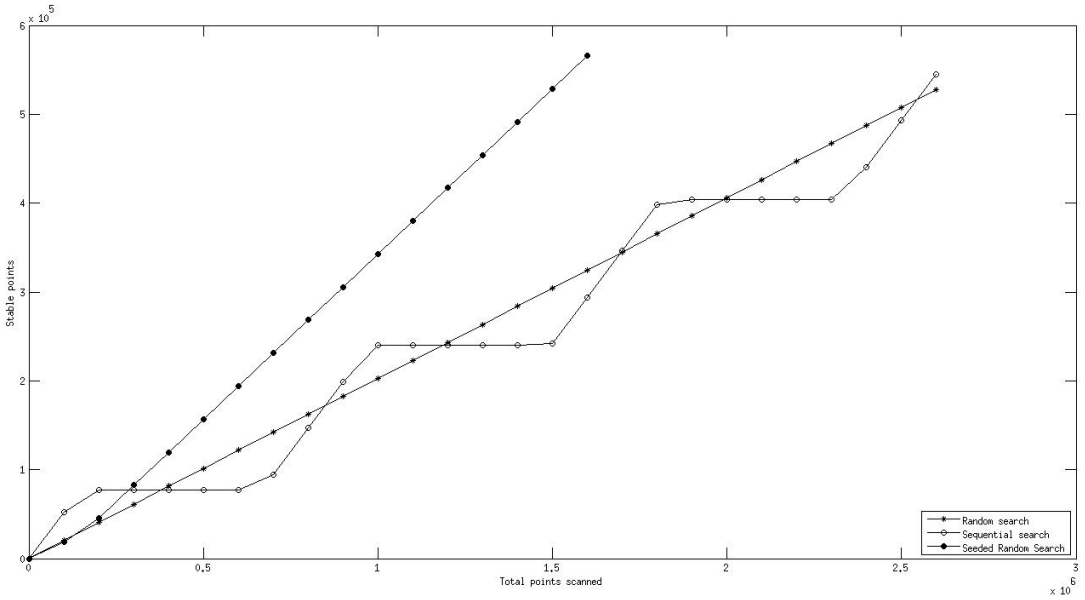

Figure 5.2: Number of stable points discovered vs total number of points examined

5,000 seed points) with the uniform distribution and the sequential search of is presented in Figure 5.2 .

Though the Poisson distribution has not been used so far, it has its applications. Given a grid over the region of $\mathbf{\Theta}$, one can use the Poisson distribution to select random grid points for evaluation. This may increase the rate of discovery of stable points. Also, one may combine the Poisson distribution with seed points from uniform distribution like we have done for the normal, and perhaps obtain a better method than even the previous one.

Chapter 6

Conclusion

The SPEs and stable filters derived thus far can convert coupled equations of motion of most systems into decoupled differential equations, which can easily be solved. This part of the project can work as an accessory for applying True Modal Control on a real-life system.

The study of stable filters thus far has just been a peek into the space of filters and automorphic transforms. While the methods and results presented here can be used for obtaining stable filters for most systems while using True Modal Control, an analytical study should prove rewarding.

6.1 Future research

Aside from applying True Modal Control to a real system, there are other avenues for academic research as well:

- The boundary of unreachable CPCs, both in the 2-dimensional and the general n-dimensional case.
- The effect of defective systems: The Jordan canonical form, and study of loosely coupled equations that the Jordan form represents. Investigate whether LAMs can be defective, and if so, explore the conditions when this may occur.
- Refining the Monte Carlo method to provide better results faster.

References

T. K. Caughey and M. E. J. O'Kelly. Classical normal modes in damped linear dynamic systems. *Journal of Applied Mechanics*, 32(3):583–588, 1965. doi: 10.1115/1.3627262. URL http://link.aip.org/link/?AMJ/32/583/1. 2

M. T. Chu and N. D. Buono. Total decoupling of general quadratic pencils, part II: Structure preserving isospectral flows. *Journal of Sound and Vibration*, 309(1-2):112 – 128, 2008a. ISSN 0022-460X. doi: 10.1016/j.jsv.2007.05.052. URL http://www.sciencedirect.com/science/article/pii/S0022460X07004245. 1, 5

M. T. Chu and N. D. Buono. Total decoupling of general quadratic pencils, part I: Theory. *Journal of Sound and Vibration*, 309(1-2):96 – 111, 2008b. ISSN 0022-460X. doi: 10.1016/j.jsv.2007.05.058. URL http://www.sciencedirect.com/science/article/pii/S0022460X07004233. 1, 3, 5, 8, 9, 10, 12, 13, 34, 36

J. Fang, Q. Li, and A. Jeary. Modified independent modal space control of m.d.o.f. systems. *Journal of Sound and Vibration*, 261(3):421 – 441, 2003. ISSN 0022-460X. doi: 10.1016/S0022-460X(02)01085-4. URL http://www.sciencedirect.com/science/article/pii/S0022460X02010854. 7

S. Garvey. Achieving stable diagonalising filters for second order systems. In *IMAC-XXVI: Conference and Exposition on Structural Dynamics - Technologies for Civil Structures*, volume 25. Society for Experimental Mechanics, 2008. 21, 22

S. Garvey, U. Prells, and M. Friswell. Diagonalising coordinate transformations for systems with general viscous damping. *Proceedings of the International Modal Analysis Conference - IMAC*, 1:622–627, 2001. URL http://www.scopus.com/inward/record.url?eid=2-s2.0-0035051399&partnerID=40&md5=3c7a57da010dcd776db7932565d83b37. cited By (since 1996) 0. 8, 9

S. Garvey, M. Friswell, and U. Prells. Co-ordinate Transformations for Second Order Systems. part I: General Transformations. *Journal of Sound and Vibration*, 258(5): 885 – 909, 2002a. ISSN 0022-460X. doi: 10.1006/jsvi.2002.5165. URL http://www.sciencedirect.com/science/article/pii/S0022460X02951655. 1, 5, 7, 8, 13

S. Garvey, M. Friswell, and U. Prells. Co-ordinate Transformations for Second Order Systems. part II: Elementary Structure-Preserving Transformations. *Journal of Sound and*

Vibration, 258(5):911 – 930, 2002b. ISSN 0022-460X. doi: 10.1006/jsvi.2002.5166. URL http://www.sciencedirect.com/science/article/pii/S0022460X02951667. 1, 5, 7, 8

P. R. Houlston. *Active Vibration Control of Rotating Machines*. PhD thesis, University of Nottingham, 2007. URL http://etheses.nottingham.ac.uk/275/. 8

D. J. Inman. Active modal control for smart structures. *Philosophical Transactions of the Royal Society of London. Series A: Mathematical, Physical and Engineering Sciences*, 359(1778):205–219, 2001. doi: 10.1098/rsta.2000.0721. URL http://rsta.royalsocietypublishing.org/content/359/1778/205.abstract. 4

S. Jiffri. *Advanced Passive and Active Methods for Vibration Control in Rotating Machines*. PhD thesis, University of Nottingham, 2011. 16, 21, 22, 29

L. Meirovitch. *Dynamics and control of structures*. Wiley-Interscience publication. Wiley, 1990. ISBN 9780471628583. URL http://books.google.com/books?id=Yz1HjDS9q2sC. 6

L. Meirovitch and G. Ryland II. Response of slightly damped gyroscopic systems. *Journal of Sound and Vibration*, 67(1):1 – 19, 1979. ISSN 0022-460X. doi: 10.1016/0022-460X(79)90497-8. URL http://www.sciencedirect.com/science/article/pii/0022460X79904978. 5

A. S. Phani. On the necessary and sufficient conditions for the existence of classical normal modes in damped linear dynamic systems. *Journal of Sound and Vibration*, 264(3):741 – 745, 2003. ISSN 0022-460X. doi: 10.1016/S0022-460X(02)01506-7. URL http://www.sciencedirect.com/science/article/pii/S0022460X02015067. 5

H. Rosenbrock. Distinctive problems of process control. *Chemical Engineering Progress*, 58(9), 1962. 6

J. Simon and S. Mitter. A theory of modal control. *Information and Control*, 13(4):316 – 353, 1968. ISSN 0019-9958. doi: 10.1016/S0019-9958(68)90834-6. URL http://www.sciencedirect.com/science/article/pii/S0019995868908346. 6

D. Watkins. *Fundamentals of Matrix Computations*. Pure and applied mathematics. John Wiley & Sons, 2010. ISBN 9780470528334. URL http://books.google.com/books?id=d0wbQwAACAAJ. 3

Appendix A

Details of Total Decoupling

In this appendix we'll present in detail the derivation of the matrices in (3.8). The classification procedure (Chu and Buono, 2008a, sec 3.1) is based upon the scaled eigenvectors $\mathbf{X}^{[1]}$, (or, equivalently, $\mathbf{Y}^{[1]}$), and divides the real eigenvalues into pairs. Let $\mathfrak{C}$, $\mathfrak{R}$ and $\mathfrak{I}$ be the index sets of complex, real and purely imaginary eigenvectors in $\mathbf{X}^{[1]}$, which provide us the index set $\mathfrak{T}$. As before, let the number of complex eigenvalues be $2p$. $\mathfrak{C}^+$ and $\mathfrak{C}^-$ are the index sets of complex-valued eigenvalues with positive and negative imaginary parts respectively. Hence, $p = n(\mathfrak{C}^+)$. $\mathfrak{T}^+$ and $\mathfrak{T}^-$ are index sets formed from the first and second values of the pairs of real eigenvalues. First, let us examine the classification of eigenvalues. The real eigenvalues $\mathbf{\Lambda}_{\mathfrak{R}}$ and $\mathbf{\Lambda}_{\mathfrak{I}}$ will be regrouped into six categories:

1. For $j = 1, \ldots, \rho$,

$$\{\mathrm{r}_j, \mathrm{i}_j\} \in \mathbf{C}_a \Leftrightarrow \lambda_{\mathrm{r}_j}\lambda_{\mathrm{i}_j} > 0 \tag{A.1}$$
$$\{\mathrm{r}_j, \mathrm{i}_j\} \in \mathbf{C}_f \Leftrightarrow \lambda_{\mathrm{r}_j}\lambda_{\mathrm{i}_j} < 0 \tag{A.2}$$

2. For $j = 1, \ldots, (n(\mathfrak{R}) - \rho)/2$,

$$\{\mathrm{r}_{\rho+2j-1}, \mathrm{r}_{\rho+2j}\} \in \mathbf{C}_b \Leftrightarrow \lambda_{\mathrm{r}_{\rho+2j-1}}\lambda_{\mathrm{i}_{\rho+2j-1}} < 0 \tag{A.3}$$
$$\{\mathrm{r}_{\rho+2j-1}, \mathrm{r}_{\rho+2j}\} \in \mathbf{C}_d \Leftrightarrow \lambda_{\mathrm{r}_{\rho+2j-1}}\lambda_{\mathrm{i}_{\rho+2j-1}} > 0 \tag{A.4}$$

3. For $j = 1, \ldots, (n(\mathfrak{I}) - \rho)/2$,

$$\{\mathrm{i}_{\rho+2j-1}, \mathrm{i}_{\rho+2j}\} \in \mathbf{C}_c \Leftrightarrow \lambda_{\mathrm{i}_{\rho+2j-1}}\lambda_{\mathrm{i}_{\rho+2j-1}} < 0 \tag{A.5}$$
$$\{\mathrm{i}_{\rho+2j-1}, \mathrm{r}_{\rho+2j}\} \in \mathbf{C}_e \Leftrightarrow \lambda_{\mathrm{i}_{\rho+2j-1}}\lambda_{\mathrm{i}_{\rho+2j-1}} > 0 \tag{A.6}$$

Collect all first indices in each $\mathbf{C}_v$ in $\mathbf{C}_v^+$ and the second indices in $\mathbf{C}_v^-$, so that $\mathbf{C}_v = \mathbf{C}_v^+ \bigcup \mathbf{C}_v^-$. Let $q_v = n(\mathbf{C}_v)/2$. Gathering the indices of real eigenvalues in $\mathfrak{T}$:

$$\mathfrak{T}^+ = \left[\mathbf{C}_a^+, \ldots, \mathbf{C}_f^+\right] \tag{A.7}$$
$$\mathfrak{T}^- = \left[\mathbf{C}_a^+, \ldots, \mathbf{C}_f^-\right] \tag{A.8}$$

Rearranging the columns of $\mathbf{I}_{2n}$ using the index order $[\mathfrak{C}^+\mathfrak{T}^+\mathfrak{C}^-\mathfrak{T}^-]$, we obtain the permutation matrix $\mathbf{P}$.

Consider the identity matrices $\mathbf{I}_a, \ldots, \mathbf{I}_f$ of size $q_a, \ldots, q_f$. Define the following block diagonal matrices:

$$\mathbf{L}^+ = diag\,[\mathbf{I}_a, \mathbf{I}_b, \iota\mathbf{I}_c, \mathbf{I}_d, -\iota\mathbf{I}_e, \mathbf{I}_f,] \tag{A.9}$$

$$\mathbf{L}^- = diag\,[\iota\mathbf{I}_a, \mathbf{I}_b, \iota\mathbf{I}_c, -\mathbf{I}_d, \iota\mathbf{I}_e, -\iota\mathbf{I}_f,] \tag{A.10}$$

$$\mathbf{R}^+ = diag\,[\mathbf{I}_a, \mathbf{I}_b, \iota\mathbf{I}_c, \mathbf{I}_d, \iota\mathbf{I}_e, \mathbf{I}_f,] \tag{A.11}$$

$$\mathbf{R}^- = diag\,[\iota\mathbf{I}_a, \mathbf{I}_b, \iota\mathbf{I}_c, \mathbf{I}_d, \iota\mathbf{I}_e, \iota\mathbf{I}_f,] \tag{A.12}$$

$$\hat{\mathbf{I}}_{n-p} = diag\,[\mathbf{I}_a, \mathbf{I}_b, -\mathbf{I}_c, \mathbf{I}_d, \mathbf{I}_e, \mathbf{I}_f,] \tag{A.13}$$

$$\tilde{\mathbf{I}}_{n-p} = diag\,[-\mathbf{I}_a, \mathbf{I}_b, -\mathbf{I}_c, -\mathbf{I}_d, -\mathbf{I}_e, \mathbf{I}_f,] \tag{A.14}$$

to obtain $\mathbf{J}_L$ and $\mathbf{J}_R$:

$$\mathbf{J}_L = \begin{bmatrix} \frac{1}{\sqrt{2}}\mathbf{I}_p & \mathbf{0} & \frac{-\iota}{\sqrt{2}}\mathbf{I}_p & \mathbf{0} \\ \mathbf{0} & \mathbf{L}^+ & \mathbf{0} & \mathbf{0} \\ \frac{1}{\sqrt{2}}\mathbf{I}_p & \mathbf{0} & \frac{\iota}{\sqrt{2}}\mathbf{I}_p & \mathbf{0} \\ \mathbf{0} & \mathbf{0} & \mathbf{0} & \mathbf{L}^- \end{bmatrix} \tag{A.15}$$

$$\mathbf{J}_R = \begin{bmatrix} \frac{1}{\sqrt{2}}\mathbf{I}_p & \mathbf{0} & \frac{-\iota}{\sqrt{2}}\mathbf{I}_p & \mathbf{0} \\ \mathbf{0} & \mathbf{R}^+ & \mathbf{0} & \mathbf{0} \\ \frac{1}{\sqrt{2}}\mathbf{I}_p & \mathbf{0} & \frac{\iota}{\sqrt{2}}\mathbf{I}_p & \mathbf{0} \\ \mathbf{0} & \mathbf{0} & \mathbf{0} & \mathbf{R}^- \end{bmatrix} \tag{A.16}$$

A cursory inspection of $\mathbf{J}_L$ and $\mathbf{J}_R$ tells us that $\mathbf{L}^+, \mathbf{L}^-, \mathbf{R}^+$, and $\mathbf{R}^-$ are used to convert the purely imaginary eigenvectors to real ones, and the other blocks of $\mathbf{J}_L$ and $\mathbf{J}_R$ deal with the complex eigenvectors. Thus, the overall effect of these matrices is a real-valued form of the eigenvectors.

$$\mathbf{A}^{[1]} = (\mathbf{Y}^{[1]}\mathbf{P}\mathbf{J}_L)^T\mathbf{A}(\mathbf{X}^{[1]}\mathbf{P}\mathbf{J}_R) = diag\left[\mathbf{I}_p, \hat{\mathbf{I}}_{n-p}, \mathbf{I}_p, \tilde{\mathbf{I}}_{n-p}\right] \tag{A.17}$$

$$\mathbf{B}^{[1]} = (\mathbf{Y}^{[1]}\mathbf{P}\mathbf{J}_L)^T\mathbf{B}(\mathbf{X}^{[1]}\mathbf{P}\mathbf{J}_R) = \begin{bmatrix} \Re\mathbf{\Lambda}_{\mathfrak{C}^+}^{-1} & \mathbf{0} & \Im\mathbf{\Lambda}_{\mathfrak{C}^+}^{-1} & \mathbf{0} \\ \mathbf{0} & \mathbf{\Omega}^+ & \mathbf{0} & \mathbf{0} \\ \Im\mathbf{\Lambda}_{\mathfrak{C}^+}^{-1} & \mathbf{0} & -\Re\mathbf{\Lambda}_{\mathfrak{C}^-}^{-1} & \mathbf{0} \\ \mathbf{0} & \mathbf{0} & \mathbf{0} & \mathbf{\Omega}^- \end{bmatrix} \tag{A.18}$$

where $\mathbf{\Omega}^+ = \mathbf{L}^+\mathbf{\Lambda}_{\mathfrak{T}^+}^{-1}\mathbf{R}^+$ and $\mathbf{\Omega}^- = \mathbf{L}^-\mathbf{\Lambda}_{\mathfrak{T}^-}^{-1}\mathbf{R}^-$.

Next we eliminate the lower-right blocks of $\mathbf{B}^{[1]}$. For this, we select an elimination matrix $\mathbf{F}$:

$$\mathbf{F} = \begin{bmatrix} \mathbf{\Phi} & \mathbf{0} & \mathbf{I}_p & \mathbf{0} \\ \mathbf{0} & \mathbf{\Psi}^+ & \mathbf{0} & \mathbf{I}_{n-p} \\ \mathbf{I}_p & \mathbf{0} & \mathbf{\Phi} & \mathbf{0} \\ \mathbf{0} & \mathbf{I}_{n-p} & \mathbf{0} & \mathbf{\Psi}^- \end{bmatrix} \tag{A.19}$$

Due to the similar block structure of $\mathbf{F}$ and $\mathbf{B}^{[1]}$, we can consider the blocks $\mathbf{\Phi}, \mathbf{\Psi}^+$ and $\mathbf{\Psi}^-$ individually. To obtain the kth diagonal entry of $\mathbf{\Phi}$:

$$\begin{bmatrix} \phi_k & 1 \\ 1 & \phi_k \end{bmatrix} \begin{bmatrix} \alpha_k & -\beta_k \\ -\beta_k & -\alpha_k \end{bmatrix} \begin{bmatrix} \phi_k & 1 \\ 1 & \phi_k \end{bmatrix} = \begin{bmatrix} \alpha_k\phi_k^2 - 2\beta_k\phi_k - \alpha_k & -\beta_k - \beta_k\phi_k^2 \\ -\beta_k - \beta_k\phi_k^2 & \alpha_k - 2\beta_k\phi_k - \alpha_k\phi_k^2 \end{bmatrix} \tag{A.20}$$

where the kth entry of $\mathbf{\Lambda}_{\mathfrak{C}^+}$ is $\alpha_k + \iota\beta_k$. [1] To eliminate the lower right element,

$$\phi_k = \frac{-\beta_k + \sqrt{\alpha_k^2 + \beta_k^2}}{\alpha_k} \tag{A.21}$$

The square root term is nothing but the absolute value of the eigenvalue in question. In terms of matrices:

$$\mathbf{\Phi} = (-\Im(\mathbf{\Lambda}_{\mathfrak{C}^+}) + abs(\mathbf{\Lambda}_{\mathfrak{C}^+}))(\Re(\mathbf{\Lambda}_{\mathfrak{C}^+}))^{-1} \tag{A.22}$$

Similarly, for $\mathbf{\Psi}^+$ and $\mathbf{\Psi}^-$,

$$\begin{bmatrix} \psi_k^+ & 1 \\ 1 & \psi_k^- \end{bmatrix} \begin{bmatrix} \omega_k^+ & 0 \\ 0 & \omega_k^- \end{bmatrix} \begin{bmatrix} \psi_K^+ & 1 \\ 1 & \psi_k^- \end{bmatrix} = \begin{bmatrix} \omega_k^+(\psi_k^+)^2 + \omega_k^- & \omega_k^+\psi_k^+ + \omega_k^-\psi_k^- \\ \omega_k^+\psi_k^+ + \omega_k^-\psi_k^- & \omega_k^-(\psi_k^-)^2 + \omega_k^+ \end{bmatrix} \tag{A.23}$$

$$\therefore \omega_k^-(\psi_k^-)^2 + \omega_k^+ = 0 \Rightarrow \psi_k^- = \pm\sqrt{-\frac{\omega_k^+}{\omega_k^-}} \tag{A.24}$$

Considering the signs in $\hat{\mathbf{I}}_{n-p}$ and $\tilde{\mathbf{I}}_{n-p}$, we can write the preceding equation in matrix form:

$$\mathbf{\Psi}^+ = \sqrt{-\mathbf{\Omega}^+(\mathbf{\Omega}^-)^{-1}} \tag{A.25a}$$

$$\mathbf{\Psi}^- = -\hat{\mathbf{I}}_{n-p}\tilde{\mathbf{I}}_{n-p}\mathbf{\Psi}^+ \tag{A.25b}$$

Having obtained $\mathbf{F}$, we only have to restore the Lancaster structure of $\mathbf{B}$. Now,

$$\mathbf{A}^{[2]} = (\mathbf{Y}^{[1]}\mathbf{P}\mathbf{J}_L\mathbf{F})^T\mathbf{A}(\mathbf{X}^{[1]}\mathbf{P}\mathbf{J}_R\mathbf{F}) = diag\left[\mathbf{A}_{11}^{[2]}, \mathbf{A}_{22}^{[2]}\right] \tag{A.26}$$

$$\mathbf{B}^{[2]} = (\mathbf{Y}^{[1]}\mathbf{P}\mathbf{J}_L\mathbf{F})^T\mathbf{B}(\mathbf{X}^{[1]}\mathbf{P}\mathbf{J}_R\mathbf{F}) = \begin{bmatrix} \mathbf{B}_{11}^{[2]} & \mathbf{B}_{12}^{[2]} \\ \mathbf{B}_{12}^{[2]} & \mathbf{0} \end{bmatrix} \tag{A.27}$$

To restore the structure, $\mathbf{A}_{22}^{[2]} = \mathbf{B}_{12}^{[2]}$. Now we employ the scaling matrix $\mathbf{\Gamma} = diag\,[\mathbf{I}_n, \mathbf{\Theta}]$,

$$\mathbf{\Theta}\mathbf{A}_{22}^{[2]}\mathbf{\Theta} = \mathbf{B}_{12}^{[2]}\mathbf{\Theta} = \mathbf{\Theta}\mathbf{B}_{12}^{[2]} \Rightarrow \mathbf{\Theta} = \mathbf{B}_{12}^{[2]}{\mathbf{A}_{22}^{[2]}}^{-1} \tag{A.28}$$

Thus we obtain the SPEs $\mathbf{\Pi}_L$ and $\mathbf{\Pi}_R$.

$$\mathbf{\Pi}_L = \mathbf{Y}^{[1]}\mathbf{P}\mathbf{J}_L\mathbf{F}\mathbf{\Gamma} \tag{A.29a}$$

$$\mathbf{\Pi}_R = \mathbf{X}^{[1]}\mathbf{P}\mathbf{J}_R\mathbf{F}\mathbf{\Gamma} \tag{A.29b}$$

[1] This is a correction of equations (34) and (35) of Chu and Buono (2008a).

Appendix B

Decoupling Algorithm

We shall present an algorithm for obtaining the diagonalized matrices directly from using only eigenvalues and not the eigenvectors. The expressions for $\mathbf{M}_D$, $\mathbf{K}_D$ and $\mathbf{C}_D$ can be derived by expanding the matrix products in (3.10). The derivations are lengthy, and not of consequence in themselves, since the matrix relations in Appendix Appendix A are far more convenient for understanding the mathematics involved. Therefore, we shall proceed directly to the expressions.

One may consult the classification of eigenvalues in Appendix A to better understand the terms used. Note that the following pseudocode begins *after* the eigensolution of the system has been obtained and the classification of eigenvalues accomplished. Since the steps for classification are obvious enough, they were not included here. Unfortunately, the classification of real eigenvalues and the operations on the resulting sets is such that the sets do not readily yield to loops.

- The eigenvalues λ_{v^+} are obtained from the corresponding index set C_{v^+}, with similar terms for C_{v^-}.
- Eigenvalue $\lambda_k = \alpha_k + \iota\beta_k$ is the kth eigenvalue in $\mathbf{\Lambda}_{\mathfrak{C}^+}$.
- The kth diagonal element in $\mathbf{M}_D$, $\mathbf{K}_D$ and $\mathbf{C}_D$ are m_k, k_k and c_k respectively.
- The kth eigenvector in $\mathbf{X}^{[1]}_{\mathfrak{C}^+}$ is $\mathbf{v}^r_k + \iota\mathbf{w}^r_k$ and $\mathbf{p}^r_k$ the kth column of $\mathbf{\Pi}_r$, with similar terms for $\mathbf{Y}^{[1]}_{\mathfrak{C}^+}$ and $\mathbf{\Pi}_l$.
- Considering a structure for $\mathbf{\Pi}_l$ and $\mathbf{\Pi}_l$ similar to the one in (3.13), so $\mathbf{p}_{v^+}$ corresponds to the position occupied by $\mathbf{X}_{C^+_v}$ for $v = a, \ldots, f$ and $\mathfrak{T}$.

begin

comment: If the denominator in any term is 0, set that term to 0

for $k = 1$ to p do

$\sigma_k \leftarrow \alpha_k^2 + \beta_k^2$

$\phi_k \leftarrow (\sqrt{\sigma_k} - \beta_k)/\alpha_k$

$t_k \leftarrow \beta_k(1 + \phi_k^2)/(\sigma_k(\phi_k^2 - 1))$

$m_k \leftarrow t_k^2(1 - \phi_k^2)$

$k_k \leftarrow \phi_k^2 - 1$

$c_k \leftarrow -4\beta_k\phi_k/\sigma_k$

$\mathbf{p}_k^r \leftarrow \sqrt{2}(\mathbf{v}_k^r\phi_k + \mathbf{w}_k^r)$

$\mathbf{p}_{k+n}^r \leftarrow \sqrt{2}t_k(\mathbf{v}_k^r + \mathbf{w}_k^r\phi_k)$

$\mathbf{p}_k^l \leftarrow \sqrt{2}(\mathbf{v}_k^l\phi_k + \mathbf{w}_k^l)$

$\mathbf{p}_{k+n}^l \leftarrow \sqrt{2}t_k(\mathbf{v}_k^l + \mathbf{w}_k^l\phi_k)$

od

$k \leftarrow p$

for $v = a$ to f do

for $i = 1$ to $n(C_v)$ do

$m_{vi} \leftarrow (\lambda_{v_i^+} + \lambda_{v_i^-})^2/\lambda_{v_i^+}^2\lambda_{v_i^-}(\lambda_{v_i^+} - \lambda_{v_i^-})$

$k_{vi} \leftarrow \lambda_{v_i^-}/\lambda_{v_i^+} - 1$

$c_{vi} \leftarrow \lambda_{v_i^-}/\lambda_{v_i^+}^2 - 1/\lambda_{v_i^-}$

if $v := b, f$

then

$m_{vi} \leftarrow -m_{vi}$

$k_{vi} \leftarrow -k_{vi}$

$c_{vi} \leftarrow -c_{ci}$

fi

$m_{k+i} \leftarrow m_{vi}$

$k_{k+i} \leftarrow k_{vi}$

$c_{k+i} \leftarrow c_{vi}$

od

$k \leftarrow k + n(C_v)$

od

for $v = a, d, f$ do

$u_v = -(\lambda_{v^+} + \lambda_{v^-})/\sqrt{\lambda_{v^+}\lambda_{v^-}}(\lambda_{v^+} - \lambda_{v^-})$

od

for $v = b, c, e$ do

$u_v = (\lambda_{v^+} + \lambda_{v^-})/\sqrt{-\lambda_{v^+}\lambda_{v^-}}(\lambda_{v^+} - \lambda_{v^-})$

od

$\mathbf{p}_{a^+}^r \leftarrow \sqrt{\lambda_{a^-}/\lambda_{a^+}}\mathbf{X}_{C_a^+} - \Im\mathbf{X}_{C_a^-}$

$\mathbf{p}_{b^+}^r \leftarrow \sqrt{-\lambda_{b^-}/\lambda_{b^+}}\mathbf{X}_{C_b^+} + \mathbf{X}_{C_b^-}$

$\mathbf{p}^r_{c^+} \leftarrow -\sqrt{-\lambda_{c^-}/\lambda_{c^+}}\Im\mathbf{X}_{C_c^+} - \Im\mathbf{X}_{C_c^-}$
$\mathbf{p}^r_{d^+} \leftarrow \sqrt{\lambda_{d^-}/\lambda_{d^+}}\mathbf{X}_{C_d^+} + \mathbf{X}_{C_d^-}$
$\mathbf{p}^r_{e^+} \leftarrow -\sqrt{\lambda_{e^-}/\lambda_{e^+}}\Im\mathbf{X}_{C_e^+} - \Im\mathbf{X}_{C_e^-}$
$\mathbf{p}^r_{f^+} \leftarrow \sqrt{-\lambda_{f^-}/\lambda_{f^+}}\mathbf{X}_{C_f^+} - \Im\mathbf{X}_{C_f^-}$
$\mathbf{p}^r_{\mathfrak{T}^+} \leftarrow \left[\mathbf{p}^r_{a^+}\ \mathbf{p}^r_{b^+}\ \mathbf{p}^r_{c^+}\ \mathbf{p}^r_{d^+}\ \mathbf{p}^r_{e^+}\ \mathbf{p}^r_{f^+}\ \right]$
$\mathbf{p}^r_{a^-} \leftarrow u_a(\mathbf{X}_{C_a^+} + \sqrt{\lambda_{a^-}/\lambda_{a^+}}\Im\mathbf{X}_{C_a^-})$
$\mathbf{p}^r_{b^-} \leftarrow u_b(\mathbf{X}_{C_b^+} + \sqrt{-\lambda_{b^-}/\lambda_{b^+}}\mathbf{X}_{C_b^-})$
$\mathbf{p}^r_{c^-} \leftarrow u_c(-\Im\mathbf{X}_{C_c^+} - \sqrt{-\lambda_{c^-}/\lambda_{c^+}}\Im\mathbf{X}_{C_c^-})$
$\mathbf{p}^r_{d^-} \leftarrow u_d(\mathbf{X}_{C_d^+} - \sqrt{\lambda_{d^-}/\lambda_{d^+}}\mathbf{X}_{C_d^-})$
$\mathbf{p}^r_{e^-} \leftarrow u_e(-\Im\mathbf{X}_{C_e^+} + \sqrt{\lambda_{e^-}/\lambda_{e^+}}\Im\mathbf{X}_{C_e^-})$
$\mathbf{p}^r_{f^-} \leftarrow u_f(\mathbf{X}_{C_f^+} - \sqrt{-\lambda_{f^-}/\lambda_{f^+}}\Im\mathbf{X}_{C_f^-})$
$\mathbf{p}^r_{\mathfrak{T}^-} \leftarrow \left[\mathbf{p}^r_{a^-}\ \mathbf{p}^r_{b^-}\ \mathbf{p}^r_{c^-}\ \mathbf{p}^r_{d^-}\ \mathbf{p}^r_{e^-}\ \mathbf{p}^r_{f^-}\right]$
$\mathbf{p}^l_{a^+} \leftarrow \sqrt{\lambda_{a^-}/\lambda_{a^+}}\mathbf{X}_{C_a^+} - \Im\mathbf{X}_{C_a^-}$
$\mathbf{p}^l_{b^+} \leftarrow \sqrt{-\lambda_{b^-}/\lambda_{b^+}}\mathbf{X}_{C_b^+} + \mathbf{X}_{C_b^-}$
$\mathbf{p}^l_{c^+} \leftarrow -\sqrt{-\lambda_{c^-}/\lambda_{c^+}}\Im\mathbf{X}_{C_c^+} - \Im\mathbf{X}_{C_c^-}$
$\mathbf{p}^l_{d^+} \leftarrow \sqrt{\lambda_{d^-}/\lambda_{d^+}}\mathbf{X}_{C_d^+} - \mathbf{X}_{C_d^-}$
$\mathbf{p}^l_{e^+} \leftarrow \sqrt{\lambda_{e^-}/\lambda_{e^+}}\Im\mathbf{X}_{C_e^+} - \Im\mathbf{X}_{C_e^-}$
$\mathbf{p}^l_{f^+} \leftarrow \sqrt{-\lambda_{f^-}/\lambda_{f^+}}\mathbf{X}_{C_f^+} + \Im\mathbf{X}_{C_f^-}$
$\mathbf{p}^l_{\mathfrak{T}^+} \leftarrow \left[\mathbf{p}^l_{a^+}\ \mathbf{p}^l_{b^+}\ \mathbf{p}^l_{c^+}\ \mathbf{p}^l_{d^+}\ \mathbf{p}^l_{e^+}\ \mathbf{p}^l_{f^+}\ \right]$
$\mathbf{p}^l_{a^-} \leftarrow u_a(\mathbf{X}_{C_a^+} + \sqrt{\lambda_{a^-}/\lambda_{a^+}}\Im\mathbf{X}_{C_a^-})$
$\mathbf{p}^l_{b^-} \leftarrow u_b(\mathbf{X}_{C_b^+} + \sqrt{-\lambda_{b^-}/\lambda_{b^+}}\mathbf{X}_{C_b^-})$
$\mathbf{p}^l_{c^-} \leftarrow u_c(-\Im\mathbf{X}_{C_c^+} - \sqrt{-\lambda_{c^-}/\lambda_{c^+}}\Im\mathbf{X}_{C_c^-})$
$\mathbf{p}^l_{d^-} \leftarrow u_e(\mathbf{X}_{C_d^+} + \sqrt{\lambda_{d^-}/\lambda_{d^+}}\mathbf{X}_{C_d^-})$
$\mathbf{p}^l_{e^-} \leftarrow u_e(\Im\mathbf{X}_{C_e^+} + \sqrt{\lambda_{e^-}/\lambda_{e^+}}\Im\mathbf{X}_{C_e^-})$
$\mathbf{p}^l_{f^-} \leftarrow u_f(\mathbf{X}_{C_f^+} + \sqrt{-\lambda_{f^-}/\lambda_{f^+}}\Im\mathbf{X}_{C_f^-})$
$\mathbf{p}^l_{\mathfrak{T}^-} \leftarrow \left[\mathbf{p}^l_{a^-}\ \mathbf{p}^l_{b^-}\ \mathbf{p}^l_{c^-}\ \mathbf{p}^l_{d^-}\ \mathbf{p}^l_{e^-}\ \mathbf{p}^l_{f^-}\right]$
for $i = 1$ to $n(\mathfrak{T}^+)$ do
    $\mathbf{p}^r_{p+i} \leftarrow \mathbf{p}^r_{\mathfrak{T}_i^+}$
    $\mathbf{p}^r_{n+p+i} \leftarrow \mathbf{p}^r_{\mathfrak{T}_i^-}$
    $\mathbf{p}^l_{p+i} \leftarrow \mathbf{p}^l_{\mathfrak{T}_i^+}$
    $\mathbf{p}^l_{n+p+i} \leftarrow \mathbf{p}^l_{\mathfrak{T}_i^-}$
od
end